Zoosyst. Evol. 98 (2) 2022, 435–453 | DOI 10.3897/zse.98.86299

# Rock island melody remastered: two new species in the *Afroedura bogerti* Loveridge, 1944 group from Angola and Namibia

Werner Conradie[1,2], Andreas Schmitz[3], Javier Lobón-Rovira[4,5,6], François S. Becker[7,8], Pedro Vaz Pinto[4,6,9,10], Morgan L. Hauptfleisch[11]

1 *Port Elizabeth Museum (Bayworld), P.O. Box 13147, Humewood 6013, South Africa*
2 *Department of Nature Conservation Management, Natural Resource Science and Management Cluster, Faculty of Science, George Campus, Nelson Mandela University, George, South Africa*
3 *Natural History Museum of Geneva, Route de Malagnou 1, C.P. 6434, 1211 Geneva 6, Switzerland*
4 *CIBIO, Centro de Investigação em Biodiversidade e Recursos Genéticos, InBIO Laboratório Associado, Campus de Vairão, Universidade do Porto, 4485-661 Vairão, Portugal*
5 *Departamento de Biologia, Faculdade de Ciências, Universidade do Porto, 4099-002 Porto, Portugal*
6 *BIOPOLIS Program in Genomics, Biodiversity and Land Planning, CIBIO, Campus de Vairão, 4485-661 Vairão, Portugal de Ciências da Educação da Huíla (ISCED-Huíla), Rua Sarmento Rodrigues, Lubango, Angola*
7 *National Museum of Namibia, Windhoek, Namibia*
8 *School of Animal, Plant and Environmental Sciences, University of the Witwatersrand, Private Bag 3, Wits 2050, Johannesburg, South Africa*
9 *Fundação Kissama, Luanda, Angola*
10 *TwinLab CIBIO/ISCED – Instituto de Ciências da Educação da Huíla, Rua Sarmento Rodrigues 2, C.P. 230, Lubango, Angola*
11 *Biodiversity Research Centre, Namibia University of Science and Technology, Windhoek, Namibia*

*https://zoobank.org/6EA087B2-3245-455F-AD10-15016E8417D3*

Corresponding author: Werner Conradie (werner@bayworld.co.za)

Academic editor: Johannes Penner ♦ **Received** 8 May 2022 ♦ **Accepted** 11 October 2022 ♦ **Published** 21 November 2022

## Abstract

Newly collected material from northern Namibia's Otjihipa Mountains and west-central Angola allowed us to revisit the *Afroedura bogerti* Loveridge, 1944 group. The employment of additional gene markers, including nuclear markers, allowed us to identify two new species in the group and infer species boundaries and potential speciation events in *Afroedura* from southwestern Africa. The new Namibian material is recovered as a sister species to *A. donveae*, from which it differs mostly by the colour of the iris (copper versus black) and dorsal colouration. Material from the first elevational gradient of the escarpment in Benguela Province, Angola was found to be more closely related to *A. bogerti* than *A. wulfhaackei*. The differences between these two species are more subtle, although the new species exhibits higher mid-body scale rows (79.5 versus 74.8), different dorsal colouration and supranasal scales always in contact (versus 57% in contact).

## Key Words

endemism, flat geckos, Gekkonidae, Reptilia, speciation

## Resumo

O material recém-colectado nas montanhas Otjihipa do norte da Namíbia e no centro-oeste de Angola permitiu-nos revisitar o grupo *Afroedura bogerti* Loveridge, 1944. O emprego de marcadores genéticos adicionais, incluindo marcadores nucleares, permitiu-nos identificar duas novas espécies no grupo e inferir limites para separar as espécies e potenciais eventos de especiação nos *Afroedura* do sudoeste Africano. O novo material da Namíbia é recuperado como espécie mais próxima de *A. donveae*, do qual difere sobretudo pela cor da iris (acobreada ao invés de negra) e pela coloração dorsal. Ao passo que o material obtido no primeiro gradiente topográfico da escarpa na

província de Benguela, Angola, revelou ser mais relacionado com *A. bogerti* do que com *A. wulfhaackei*. As diferenças entre estas duas espécies são mais subtis, muito embora as novas espécies axibam maior número de escamas a meio do corpo (79.5 em vez de 74.8), diferente coloração dorsal e escamas supranasais sempre em contacto (em vez de apenas em contacto em 57%).

## Palavras-chave

endemismo, especiação, Gekkonidae, Osga-achatada, Reptilia

## Introduction

African flat geckos *Afroedura* Loveridge, 1944 currently comprise 32 species (Uetz et al. 2022), occurring from western Angola southwards to South Africa and along the eastern escarpment northwards to central Mozambique (Jacobsen et al. 2014; Branch et al. 2017, 2021). In recent years there has been a considerable increase in the number of new *Afroedura* species described from Angola (Branch et al. 2021), Mozambique (Branch et al. 2017) and the northern provinces of South Africa (Jacobsen et al. 2014). Numerous additional candidate new species have been identified and await formal description (Makhubo et al. 2015; Busschau et al. 2019).

Until recently, only three species of *Afroedura* had been recorded from Namibia and Angola, namely *A. africana* (Boulenger, 1888), *A. tirasensis* Haacke, 1965 and *A. bogerti* Loveridge, 1944. However, a recent revision of Angolan material of the *A. bogerti*-group (Branch et al. 2021), revealed cryptic diversity and increased the total number to five species for the country: *A. bogerti* Loveridge, 1944, *A. wulfhaackei* Branch, Schmitz, Lobón-Rovira, Baptista, António, Conradie, 2021, *A. donveae* Branch, Schmitz, Lobón-Rovira, Baptista, António, Conradie, 2021, *A. preadicta* Branch, Schmitz, Lobón-Rovira, Baptista, António, Conradie, 2021, and *A. vazpintorum* Branch, Schmitz, Lobón-Rovira, Baptista, António, Conradie, 2021. These Angolan species were grouped in two genetic clusters: south-western coastal low-lying (*A. donveae*, *A. vazpintorum* [with an isolated southern escarpment population], *A. praedicta*) and inland central high-lying (*A. wulfhaackei*, *A. bogerti*). All species are currently regarded as Angolan endemics. In both wide-ranging species, *A. vazpintorum* and *A. wulfhaackei*, genetic sub-structuring was documented (Branch et al. 2021). In *A. vazpintorum* two subclades were identified, which differed by an average 4.1% for the *16S* mitochondrial marker. One subclade was found to be widely distributed across much of the semi-arid 'Pro-Namib' coastal zone north of Moçâmedes, while the other subclade was restricted to the Humpata plateau. What complicated the matter further was that a sample collected syntopic with other Humpata samples was imbedded in the coastal clade and no morphological differences were observed. On the other hand, in *A. wulfhaackei* four subclades were identified that differed genetically by a similar margin from the previous species (3.3–4.2% *16S*), with once again no clear morphological differences. Follow-up work with more material and gene coverage was recommended to resolve this issue.

Unfortunately, the status of historical records of *A. bogerti* from northern Namibia (see Branch 1998; Griffin, 2002) could not be assessed together with the Angolan material given the lack of fresh material suitable for inclusion in a phylogenetic analysis. During recent expeditions new material was collected in northern Namibia and Angola, giving the opportunity to revisit this group in more detail. In this study we build on the previous work of Branch et al. (2017, 2021) by adding additional samples and gene markers to infer species boundaries and potential speciation events within the *A. bogerti*-group in south-western Africa. This allowed us to look a bit deeper into the genetic sub-structuring documented in the two widespread species, *A. vazpintorum* and *A. wulfhaackei*.

## Materials and methods

### Sampling

The material used in Branch et al. (2021) was supplemented with sequences from additional genes, as well as with newly-collected samples from Otjihipa Mountains, northern Namibia (n = 2) and Angola (n = 17) (see Table 1, Fig. 1). Specimens were collected and processed following the protocols described in Branch et al. (2021). Newly collected voucher specimens were deposited in the natural history collections of the National Museum of Namibia, Windhoek (NMNW) and Fundação Kissama (FKH), Luanda, Angola.

### DNA extraction, amplification and sequencing

Total genomic DNA for the new samples was extracted from tissue samples using the E.Z.N.A. Tissue DNA Kit (VWR/Omega bio-tek) and the Qiagen DNeasy Tissue Kit, following the manufacturer's protocols. The following genes were amplified: two partial mitochondrial ribosomal genes (ribosomal ribonucleic acid [*12S* and *16S*]), two partial mitochondrial genes (cytochrome b [*Cyt-b*] and NADH-dehydrogenase subunit 2 [*ND2*]) and two partial nuclear gene (oocyte maturation factor [*c-mos*] and recombination activating protein [*RAG1*]). Respective primers and reference to PCR protocols are given in Table 2. PCR products

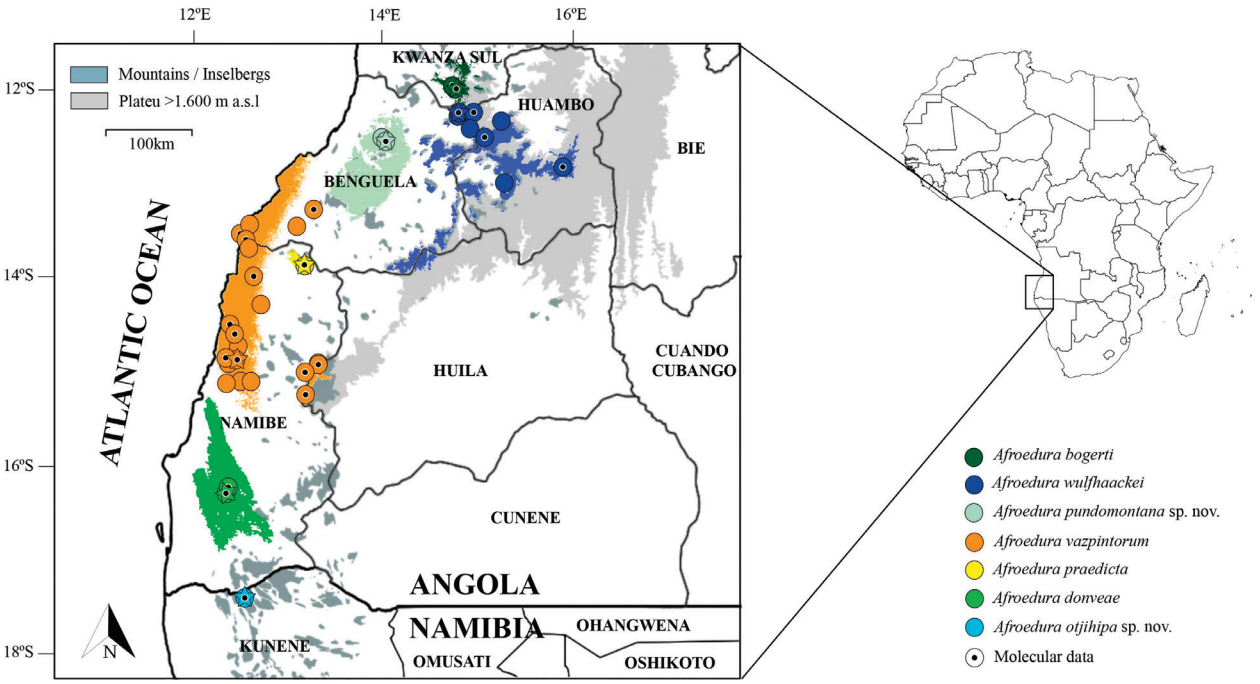


**Figure 1.** All occurrence records (coloured circles) and predicted distribution for the *Afroedura bogerti* group from southwestern Africa. No predicted distribution could be created for *A. othjihipa* sp. nov. Angolan provinces and Namibian regions are labelled accordingly. Stars represent the respective type localities and black dots with white borders represent localities used in the phylogenetic analysis.

**Table 1.** *Afroedura* specimens with generalised localities and GenBank accession numbers of vouchers used in this study. *Additional samples added during this study. ANG/AG – William R. Branch field numbers; CHL – Colecção Herpetológica do Lubango (CHL), Instituto Superior de Ciências de Educação da Huíla (ISCED-Huíla), Angola; FKH – Fundação Kissama, Luanda, Angola; JLRZC – Javier Lobón-Rovira field numbers; KTH – Krystal Tolley field numbers; NB – Ninda Baptista field numbers; NMNW – National Museum of Namibia, Windhoek; P – Pedro Vaz Pinto field numbers; PEM – Port Elizabeth Museum, South Africa; WC – Werner Conradie field numbers; ZMB – Museum für Naturkunde, Berlin, Germany. SC – subclade.

| Species | Locality | Sample Number | Museum Number | *16S* | *12S* | *c-mos* | *RAG1* | *Cyt-b* | *ND2* |
|---|---|---|---|---|---|---|---|---|---|
| *A. praedicta* | Serra da Neve, Angola | NB 853 | ZMB 91607 | MW354010 | OP653587 | OP686766 | OP686640 | OP686714 | OP686613 |
| *A. praedicta* | Serra da Neve, Angola | NB 854 | CHL 854 | MW354011 | OP653588 | OP686767 | OP686641 | OP686715 | OP686614 |
| *A. praedicta* | Serra da Neve, Angola | NB 855 | CHL 855 | MW354012 | OP653589 | OP686768 | OP686642 | NA | OP686615 |
| *A. otjihipa* sp. nov. | Otjihipa, Namibia | SMR 11182* | NMNW R11253 | OP653544 | NA | OP686789 | OP686638 | NA | OP686623 |
| *A. otjihipa* sp. nov. | Otjihipa, Namibia | SMR 11183* | NMNW R11254 | OP653545 | NA | OP686790 | OP686639 | NA | OP686624 |
| *A. donveae* | Omauha Lodge, Angola | E259.17/KTH09-196 | PEM R17936 | LM993776 | OP653553 | OP686732 | OP686633 | NA | OP686594 |
| *A. donveae* | Omauha Lodge, Angola | E259.18/KTH09-197 | PEM R17937 | LM993777 | OP653554 | OP686733 | OP686634 | NA | OP686595 |
| *A. donveae* | Omauha Lodge, Angola | P9-284 | Na | MW354008 | OP653602 | OP686780 | OP686635 | NA | OP686621 |
| *A. donveae* | Omauha Lodge, Angola | P9-285 | Na | MW354009 | OP653603 | OP686781 | OP686636 | NA | OP686622 |
| *A. vazpintorum* SC1 | 52 km north on tar road on road to Lucira, Angola | E259.12/ANG 311 | PEM R21596 | MF565461 | OP653548 | OP686727 | OP686644 | OP686685 | NA |
| *A. vazpintorum* SC1 | 1 km east of Farm Mucungo, Angola | E259.13/AG 138 | PEM R24115 | MF565463 | OP653549 | OP686728 | OP686645 | OP686686 | OP686590 |
| *A. vazpintorum* SC1 | 1 km east of Farm Mucungo, Angola | E259.14/AG 137 | PEM R24114 | MF565460 | OP653550 | OP686729 | OP686646 | OP686687 | OP686591 |
| *A. vazpintorum* SC1 | 1 km east of Farm Mucungo, Angola | E259.15/AG 141 | PEM R24118 | MF565462 | OP653551 | OP686730 | OP686647 | OP686688 | OP686592 |
| *A. vazpintorum* SC1 | 10.4 km south of Rio Mucungo on tar road to Bentiaba, Angola | E260.12/samp39 | Na | MF565459 | OP653560 | OP686739 | OP686650 | OP686693 | OP686598 |
| *A. vazpintorum* SC1 | 10.4 km south of Rio Mucungo on tar road to Bentiaba, Angola | E260.13/samp57 | PEM R24203 | MF565458 | OP653561 | OP686740 | OP686651 | OP686694 | OP686599 |
| *A. vazpintorum* SC1 | 10.4 km south of Rio Mucungo on tar road to Bentiaba, Angola | E260.14/samp58 | PEM R24204 | MF565457 | OP653562 | OP686741 | OP686652 | OP686695 | OP686600 |
| *A. vazpintorum* SC1 | 20 km south Bentiaba, Angola | E260.15/samp62 | PEM R24219 | MF565456 | OP653563 | OP686742 | OP686653 | NA | OP686601 |
| *A. vazpintorum* SC1 | approx. 18 km E Lucira, Angola | NB 834 | CHL 834 | MW354019 | OP653585 | OP686764 | OP686658 | OP686712 | OP686611 |
| *A. vazpintorum* SC1 | approx. 18 km E Lucira, Angola | NB 835 | CHL 835 | MW354020 | OP653586 | OP686765 | OP686659 | OP686713 | OP686612 |
| *A. vazpintorum* SC1 | Mariquita, Angola | P9-154 | Na | MW354018 | OP653601 | OP686779 | OP686666 | NA | NA |
| *A. vazpintorum* SC1 | 50 km east Namibe on main tar road to Leba, Angola | E259.16/ANG 289 | PEM R21595 | MF565454 | OP653552 | OP686731 | OP686648 | NA | OP686593 |
| *A. vazpintorum* SC1 | Bimbe, Estação Zootecnica, Angola | NB 743 | CHL 743 | MW354017 | OP653578 | OP686757 | OP686654 | NA | OP686607 |
| *A. vazpintorum* SC1 | Tundavala, Angola | P0-103* | Na | OP653527 | OP653590 | OP686769 | OP686660 | NA | OP686616 |
| *A. vazpintorum* SC1 | Tundavala, Angola | P0-104* | FKH-0518 | OP653528 | OP653591 | NA | OP686661 | NA | OP686617 |
| *A. vazpintorum* SC1 | Meva Beach, Angola | E259.9/samp30 | PEM R22488 | MF565455 | OP653556 | OP686735 | OP686649 | NA | NA |

| Species | Locality | Sample Number | Museum Number | *16S* | *12S* | *c-mos* | *RAG1* | *Cyt-b* | *ND2* |
|---|---|---|---|---|---|---|---|---|---|
| *A. vazpintorum* SC1 | Carivo, Angola | P8-19 | Na | MW354015 | OP653598 | OP686776 | OP686664 | NA | OP686620 |
| *A. vazpintorum* SC1 | Carivo, Angola | P8-20 | Na | MW354016 | OP653599 | OP686777 | OP686665 | NA | NA |
| *A. vazpintorum* SC2 | Bimbe, Estação Zootecnica, Angola | NB 744* | CHL 744 | OP653529 | OP653579 | OP686758 | OP686655 | OP686707 | OP686608 |
| *A. vazpintorum* SC2 | Bimbe, Estação Zootecnica, Angola | NB 745 | CHL 745 | MW354013 | OP653580 | OP686759 | OP686656 | OP686708 | OP686609 |
| *A. vazpintorum* SC2 | Bimbe, Estação Zootecnica, Angola | NB 746 | CHL 746 | MW354014 | OP653581 | OP686760 | OP686657 | OP686709 | OP686610 |
| *A. vazpintorum* SC2 | Tchivinguiro, Angola | P0-97* | FKH0514 | OP653530 | OP653596 | OP686774 | OP686662 | OP686716 | OP686618 |
| *A. vazpintorum* SC2 | Tchivinguiro, Angola | P0-98* | FKH0515 | OP653531 | OP653597 | OP686775 | OP686663 | OP686717 | OP686619 |
| *A. pundomontana* sp. nov. | Alto Pundo – Bocoio, Angola | WC-6524* | PEM R24743 | OP653543 | NA | OP686791 | OP686643 | NA | OP686625 |
| *A. pundomontana* sp. nov. | Alto Pundo – Bocoio, Angola | P1-280* | FKH0688 | OP653532 | OP653607 | OP686785 | NA | OP686722 | NA |
| *A. pundomontana* sp. nov. | Alto Pundo – Bocoio, Angola | P1-281* | FKH0689 | OP653533 | OP653608 | OP686786 | NA | OP686723 | NA |
| *A. pundomontana* sp. nov. | Alto Pundo – Bocoio, Angola | P1-282* | FKH0690 | OP653534 | OP653609 | OP686787 | NA | OP686724 | NA |
| *A. bogerti* | Farm Namba , Angola | E260.1/samp23 | PEM R24184 | MF565467 | OP653557 | OP686736 | OP686626 | OP686690 | OP686597 |
| *A. bogerti* | Farm Namba, Angola | E260.2/samp24 | PEM R24185 | MF565468 | OP653568 | OP686747 | OP686627 | OP686700 | OP686602 |
| *A. bogerti* | Farm Namba, Angola | E260.3/samp25 | PEM R24186 | MF565466 | OP653569 | OP686748 | OP686628 | OP686701 | OP686603 |
| *A. bogerti* | 400 m north of Mission de Namba grounds, Angola | E260.4/samp27 | PEM R24187 | MF565465 | OP653570 | OP686749 | OP686629 | NA | OP686604 |
| *A. bogerti* | 400 m north of Mission de Namba grounds, Angola | E260.5/samp28 | Na | MF565464 | OP653571 | OP686750 | OP686630 | OP686702 | OP686605 |
| *A. bogerti* | Namba, Angola | JLRZC0015 | Na | MW354021 | P653576 | OP686755 | OP686631 | NA | NA |
| *A. bogerti* | Namba, Angola | JLRZC0016 | Na | MW354022 | OP653577 | OP686756 | OP686632 | NA | OP686606 |
| *A. bogerti* | Namba, Angola | P1-286* | Na | OP653535 | OP653610 | OP686788 | NA | NA | NA |
| *A. wulfhaackei* SC1 | Farm Victoria-Verdun, 2 km S of Mt. Sandula, Angola | E260.6/samp31 | Na | MF565470 | OP653572 | OP686751 | OP686675 | OP686703 | NA |
| *A. wulfhaackei* SC1 | Farm Victoria-Verdun, 2 km S of Mt. Sandula, Angola | E260.7/samp32 | Na | MF565469 | OP653573 | OP686752 | OP686676 | OP686704 | NA |
| *A. wulfhaackei* SC1 | Farm Victoria-Verdun, 2 km S of Mt. Sandula, Angola | E260.8/samp33 | PEM R24191 | MF565471 | OP653574 | OP686753 | OP686677 | OP686705 | NA |
| *A. wulfhaackei* SC1 | Farm Victoria-Verdun, 2 km S of Mt. Sandula, Angola | E260.9/samp34 | PEM R24192 | MF565469 | OP653575 | OP686754 | OP686678 | OP686706 | NA |
| *A. wulfhaackei* SC1 | Sandula, Angola | P9-141 | | MW354023 | OP653600 | OP686778 | OP686682 | OP686718 | NA |
| *A. wulfhaackei* SC1 | Moco - Kapa Kuito, Angola | P0-49* | FKH-0472 | OP653536 | OP653592 | OP686770 | NA | NA | NA |
| *A. wulfhaackei* SC2 | 5 km southwest of Lepi, Angola | E260.11/samp37 | PEM R24201 | MF565472 | OP653559 | OP686738 | OP686670 | OP686692 | NA |
| *A. wulfhaackei* SC2 | Lepi, Angola | P1-162* | FKH-0593 | OP653537 | OP653604 | OP686782 | NA | OP686719 | NA |
| *A. wulfhaackei* SC2 | Lepi, Angola | P1-163* | FKH-0594 | OP653538 | OP653605 | OP686783 | NA | OP686720 | NA |
| *A. wulfhaackei* SC2 | Lepi, Angola | P1-164* | FKH-0595 | O653539 | OP653606 | OP686784 | NA | OP686721 | NA |
| *A. wulfhaackei* SC3 | Candumbo Rocks Memorial, Angola | E259.10/WC-4037 | PEM R22490 | MF565474 | OP653546 | OP686725 | OP686667 | OP686683 | NA |
| *A. wulfhaackei* SC3 | Candumbo Rocks Memorial, Angola | E259.11/WC-4038 | PEM R22491 | MF565475 | OP653547 | OP686726 | OP686668 | OP686684 | NA |
| *A. wulfhaackei* SC3 | Candumbo Rocks Memorial, Angola | E260.10/samp35 | PEM R24200 | MF565473 | OP653558 | OP686737 | OP686669 | OP686691 | NA |
| *A. wulfhaackei* SC4 | Maka-Mombolo, north-east of Balombo, Angola | E260.16/samp70 | PEM R24236 | MF565476 | OP653564 | OP686743 | OP686671 | OP686696 | NA |
| *A. wulfhaackei* SC4 | 5 km west of Maka-Mombolo, Angola | E260.17/samp71 | PEM R24232 | MF565477 | OP653565 | OP686744 | OP686672 | OP686697 | NA |
| *A. wulfhaackei* SC4 | 5 km west of Maka-Mombolo, Angola | E260.18/samp72 | PEM R24233 | MF565478 | OP653566 | OP686745 | OP686673 | OP686698 | NA |
| *A. wulfhaackei* SC4 | 5 km west of Maka-Mombolo, Angola | E260.19/samp73 | PEM R24234 | MF565479 | OP653567 | OP686746 | OP686674 | OP686699 | NA |
| *A. wulfhaackei* SC4 | Morro do Moco, camp near Canjonde, Angola | NB 817 | CHL 817 | MW354024 | OP653582 | OP686761 | OP686679 | OP686710 | NA |
| *A. wulfhaackei* SC4 | Morro do Moco, camp near Canjonde, Angola | NB 818 | CHL 818 | MW354025 | OP653583 | OP686762 | OP686680 | OP686711 | NA |
| *A. wulfhaackei* SC4 | Morro do Moco, camp near Canjonde, Angola | NB 819 | CHL 819 | MW354026 | OP653584 | OP686763 | OP686681 | NA | NA |
| *A. wulfhaackei* SC4 | Moco - Kapa Kuito, Angola | P0-50* | FKH-0473 | OP653540 | OP653593 | OP686771 | NA | NA | NA |
| *A. wulfhaackei* SC4 | Moco - Kapa Kuito, Angola | P0-51* | FKH-0474 | OP653541 | OP653594 | OP686772 | NA | NA | NA |
| *A. wulfhaackei* SC4 | Moco - Kapa Kuito, Angola | P0-52* | FKH-0475 | OP653542 | OP653595 | OP686773 | NA | NA | NA |
| *A. loveridgei* | Near Moatize, Tete Province, Mozambique | EI 123 | | MF565446 | OP653555 | OP686734 | OP686637 | OP686689 | OP686596 |
| *A. karroica* (outgroup) | Eastern Cape Province, 41km SE Murraysburg, South Africa | | PEM FN1112 | LM993744 | NA | JQ945523 | KM073485 | NA | JX041302 |

were sequenced at Macrogen Corp. (Amsterdam, Netherlands). For quality assurance, both directions of the amplified PCR products were sequenced. For the molecular comparisons, newly-sequenced vouchers (n = 19) were used as well as extending previously used samples (n = 48; used for the previously published *16S* sequences [Branch et al. 2017, 2021]) for five additional genes. The final dataset comprised 68 ingroup samples from different localities covering the entire distribution of Angolan and Namibian *Afroedura* '*bogerti*' populations and *Afroedura karroica* as outgroup. Locality data and respective GenBank (https://www.ncbi.nlm.nih.gov/genbank/; Benson et al. 2013) numbers for each sample are listed in Table 1.

## Phylogenetic analysis

Sequences were checked for reliability using the original chromatograph data in the program BioEdit v.7.2.5 (Hall 1999), aligned using ClustalX v.1.6 (Thompson et al. 1997), with each alignment then checked manually for

**Table 2.** The primers and final sequence lengths for the two nuclear genes and four mitochondrial genes used in this study.

| Gene | Sequence length (bp) | Primer | Sequence (5' -> 3') | Reference |
|---|---|---|---|---|
| *16S* | 594 | 16Sa | CGC CTG TTT ATC AAA AAC AT | Palumbi et al. 1991 |
| | | 16Sb | CCG GTC TGA ACT CAG ATC ACG T | Palumbi et al. 1991 |
| *C-mos* | 399 | CmosG73 | GCG GTA AAG CAG GTG AAG AAA | Wiens et al. 2010 |
| | | CmosG74 | TGA GCA TCC AAA GTC TCC AAT C | Wiens et al. 2010 |
| *Cyt-b* | 1008 | CytBL14910 | GAC CTG TGA TMT GAA AAC CAY CGT TGT | Burbrink et al. 2000 |
| | | CytBH16064 | CTT TGG TTT ACA AGA ACA ATG CTT TA | Burbrink et al. 2000 |
| *RAG1* | 639 | RAG1F700 | GGA GAC ATG GAC ACA ATC CAT CCT AC | Bauer et al. 2007 |
| | | RAG1R700 | TTT GTA CTG AGA TGG ATC TTT TTG CA | Bauer et al. 2007 |
| *ND2* | 1014 | ND2L4437R | AAG CTT TCG GGC CCA TAC C | Stanley et al. 2011 |
| | | ND2H5540F | TTT AGG GCT TTG AAG GC | Bauer et al. 2010 |
| | | ND2R102 | CAG CCT AGG TGG GCG ATT G | Bauer et al. 2010 |
| *12S* | 437 | 12sf700 | AAA CTG GGA TTA GAT ACC CCA CTA T | Stanley et al. 2011 |
| | | 12sr600 | GAG GGT GAC GGC GGT GTG T | Stanley et al. 2011 |

errors. Protein-coding partitions of mitochondrial (*Cyt-b*, *ND2*) and nuclear genes (*c-mos*, *RAG1*), were translated to amino acids with the program Geneious Prime v.2021.2.2 (https://www.geneious.com) to set codon positions and confirm absence of stop codons. The final alignment of all six genes, including nuclear and mitochondrial loci, consisted of 4091 base pairs. Sequence lengths are detailed in Table 2.

Two techniques for phylogenetic estimation were applied: Bayesian Inference (BI) using MrBayes v.3.26 (Ronquist et al. 2012) and Maximum Likelihood (ML) using IQ-Tree v.2.1.2 (Nguyen et al. 2015; Minh et al. 2020) as implemented in PhyloSuit v.1.2.2 (Zhang et al. 2020) using the ultrafast bootstrap option. Both BI and ML used the recognised partition schemes identified with PartitionFinder 2 (Lanfear et al. 2016) as implemented in PhyloSuit v.1.2.2. Partitioning schemes and substitution models are provided in Table 3.

**Table 3.** Partition schemes and models of substitution for the Bayesian (PP) and maximum-likelihood (ML) calculations.

| Substitution model | Included partitions |
|---|---|
| 1 GTR + I + G | *12S*, *16S*, *ND2* (P1), *Cyt-b* (P1) |
| 2 HKY + I | *RAG1* (P1, P2, P3), *c-mos* (P1, P2. P3) |
| 3 HKY + I + G | *ND2* (P2), *Cyt-b* (P2) |
| 4 TrN + G | *ND2* (P3), *Cyt-b* (P3) |

Support values for the two phylogenetic approaches were calculated. Bootstrap analyses (BS) with 50000 ultrafast bootstraps evaluated the relative branch support in the ML analysis. As we used the ultrafast bootstrap option, only clades with support ≥ 95% were considered strongly supported. Bayesian analyses were run under partitioned schemes for 50 million generations with four chains sampled every 1000 generations, with a burn-in of 10000 trees. Clades with posterior probabilities (PP) ≥ 0.95 were considered strongly supported. Convergence and mixing of the parameters for each run of the Bayes analysis was checked with the Effective Samples Size (ESS) using Tracer v.1.72 (Rambaut et al. 2018). The final trees were visualised with FigTree v.1.4.4 (Rambaut 2014; http://tree.bio.ed.ac.uk/software/figtree/). Uncorrected p-distances between operational taxonomical units (OTUs) and within OTUs were calculated with MEGA X v.11.0.8 (Kumar et al. 2018) for the partial *16S* gene as these values were often used to prove distinctness at the species level in *Afroedura* (Branch et al. 2017, 2021).

## Morphology

We examined newly collected material in the collections of the National Museum of Namibia (NMNW), Windhoek, Namibia and Fundação Kissama (FKH), Luanda, Angola. The following characters were assessed: 1) presence or absence of internasal granules between the supranasal scales; 2) number of postmental scales; 3) number of scales in contact in a straight line between the anterior corners of eyes across the crown of the head; 4) number of scales between upper edge of earhole and rear margin of eye counted along the shortest distance between them; 5) number of scales between nostril and front edge of orbit, including postnasal; 6) number of enlarged supralabials to the angle of the jaw at midorbital position; 7) number of enlarged infralabials to the angle of the jaw at midorbital position; 8) number of midbody scale rows (MSR), counted at the widest part of the trunk; 9) number of scale rows on dorsal surface per tail whorl (counted 3–6 verticils posterior to the cloaca); 10) number of scales rows on ventral surface per tail whorl (counted 3–6 verticils posterior to the cloaca); and 11) number of precloacal pores in males. In Branch et al. (2021) it was erroneously recorded that the nostril is in direct contact with the rostral in all species in the *A. bogerti*-group. The nostril is actually pierced between the first supralabial and three nasal scales, and is narrowly excluded from the rostral. We here rectify this mistake by updating the diagnosis of the group (see Taxonomy).

The following measurements were taken in millimeters (mm) using a digital calliper (accuracy of 0.01 mm) with the aid of a Nikon SMZ1270 dissecting microscope: 1) snout-vent length (SVL – from the tip of the snout to the cloaca with the gecko flattened on its back), 2) tail length (TL, only original tails were measured); 3) head length (HL – tip of snout to retro-articular process of jaw); 4) head width (HW – widest point of head approximately at the level of eyes); 5) snout length (SL – tip of snout to front of orbit); 6) eye diameter (ED – measured in horizontal orientation); 7) ear to eye length (EE – top edge of earhole to back of eye); 8) ear opening (EO –

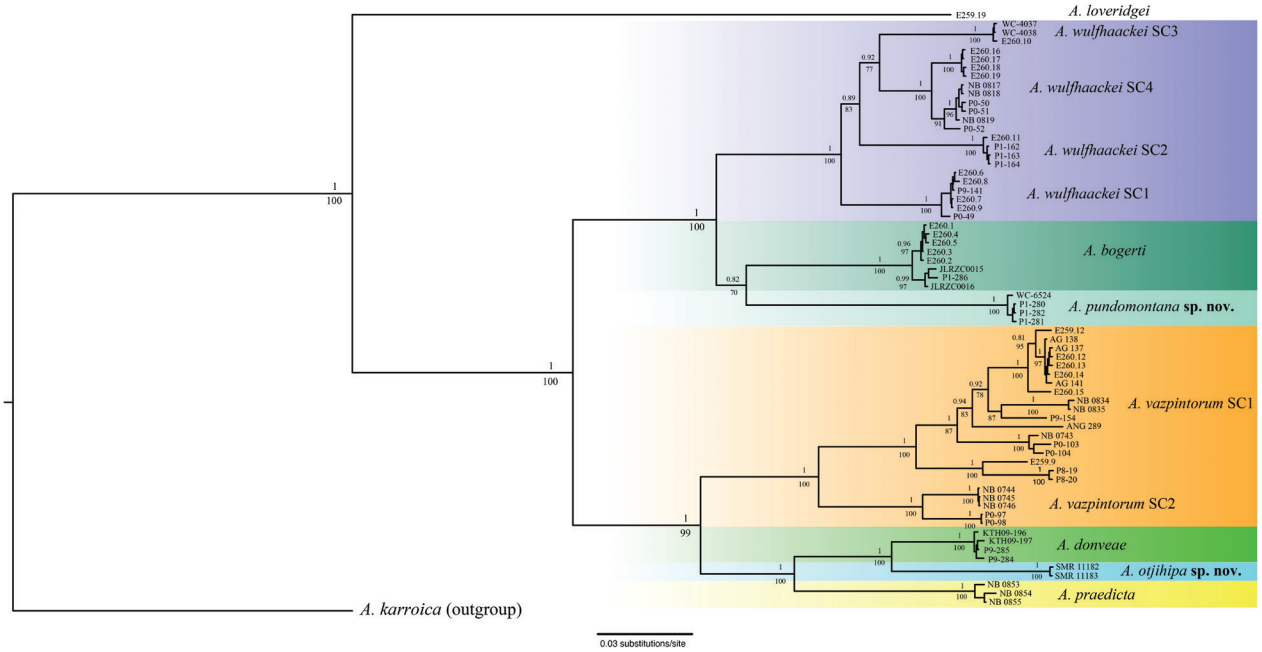


**Figure 2.** Phylogenetic tree topology based on the combined mitochondrial (*12S*, *16S*, *Cyt-b*, *ND2*) and nuclear (*c-mos*, *RAG1*) genes, using *Afroedura karroica* as outgroup. Support values for Bayesian posterior probabilities (above nodes) and maximum likelihood bootstraps (below nodes) are indicated in the tree (shown values: ML: ≥ 70% / PP: ≥ 0.75).

greatest length); and 9) internostril distance (IN – shortest distance between nostrils). All head measurements were done on the right side of the head.

## Predicted species distribution mapping

Due to the low number of occurrence records we produce predicted distribution maps for each species in the *A. bogerti*-group by performing species distribution models (SDM) based on suitable bioclimatic areas using Maxent (Yang et al. 2013). The model included a buffer of 2 degrees (~250 km) from the most peripheral observations of *A. bogerti*-group species (Branch et al. 2021). Nineteen bioclimatic variables were obtained from the WorldClim data set (Fick and Hijmans 2017; http://www.worldclim.org/) at a spatial resolution of 30 arc-second (~1 km$^2$). For those variables, we ran a correlation model to eliminate collinearity between variables in the sampled area and within sample points (Candau and Fleming 2005), and variables with correlation coefficient ≥ 0.7 were selected in order to capture all the bioclimatic range over the distribution of the species (Enriquez-Urzelai et al. 2019; Branch et al. 2021). Therefore, the variables included for analysis were: mean diurnal temperature range (Bio1); maximum temperature of the warmest month (Bio5), minimum temperature of the coldest month (Bio6); annual precipitation (Bio12); precipitation seasonality (Bio15), and precipitation of wettest quarter (Bio16). Given the small sample size for some species, we ran a cross-validation model, which utilises all the samples except for leaving out one sample in each run (Bittencourt-Silva et al. 2016; Branch et al. 2021), and hinge features only with the regularisation parameter set to 2.5 to produce smoother response curves and reduce overfitting (Briscoe et al. 2016). The final maps were generated selecting areas with more than 90% of climate suitability for each species with the exception of "*Afroedura* sp. 2" for which the sample size was too low to run a SDM.

# Results

## Molecular analyses

Molecular analyses concur with previously published results on the Angolan members of the genus *Afroedura* (Branch et al. 2017, 2021). The ESS values for the combined Bayes analysis were well above the recommended 200 threshold, thus indicating that the burn-in was sufficient and convergence was achieved. The addition of five new genes strengthened node support on all levels, with the two nuclear genes especially adding support for the deeper nodes form both the BI and ML trees. In addition to the previously identified five genetically supported clades of Angolan *Afroedura*, analysis of our additional material resulted in the recognition of two further well-supported clades, namely *Afroedura* sp. 1 from Bocoio, Angola and *Afroedura* sp. 2 from Otjihipa, Namibia (Fig. 2). In both new clades we observe only very low intraspecific differences, but comparatively high interspecific differences, compared to both the two widespread species and the other major clades of Angolan *Afroedura* (Table 4), but this low intraspecific variation can also be due to sampling localities of the vouchers being either identical or very close to each other (Table 1). Individual analyses of

**Table 4.** Summary of intra- and interclade uncorrected pairwise sequence divergences (%) for specimens of *Afroedura* clades compared to *A. loveridgei* for *16S* rRNA. Interclade distances below 5% (see the relevant discussion in the main text) are marked in bold. SC – subclades.

| | Intraclade distances | *A. loveridgei* | *A. bogerti* | *A. donveae* | *A. praedicta* | *A. pundomontana* sp. nov. | *A. otjihipa* sp. nov. | *A. vazpintorum* SC1 | *A. vazpintorum* SC2 | *A. wulfhaackei* SC1 | *A. wulfhaackei* SC2 | *A. wulfhaackei* SC3 | *A. wulfhaackei* SC4 |
|---|---|---|---|---|---|---|---|---|---|---|---|---|---|
| ***A. loveridgei*** | - | - | | | | | | | | | | | |
| ***A. bogerti*** | 0.2 | 17.2 | - | | | | | | | | | | |
| ***A. donveae*** | 0.1 | 19.6 | 10.7 | - | | | | | | | | | |
| ***A. praedicta*** | 0.7 | 17.5 | 8.8 | 6.5 | - | | | | | | | | |
| ***A. pundomontana* sp. nov.** | 0.1 | 17.8 | 7.8 | 12.1 | 11.0 | - | | | | | | | |
| ***A. otjihipa* sp. nov.** | 0.0 | 17.3 | 11.0 | 7.4 | 7.9 | 13.1 | - | | | | | | |
| ***A. vazpintorum* SC1** | 2.2 | 18.0 | 11.0 | 8.8 | 8.4 | 11.6 | 11.8 | - | | | | | |
| ***A. vazpintorum* SC2** | 1.0 | 17.3 | 9.5 | 8.9 | 7.6 | 10.6 | 10.9 | **4.6** | - | | | | |
| ***A. wulfhaackei* SC1** | 0.1 | 14.9 | 6.4 | 10.0 | 9.6 | 9.3 | 11.2 | 10.5 | 9.9 | - | | | |
| ***A. wulfhaackei* SC2** | 0.1 | 15.5 | 6.7 | 10.2 | 9.1 | 9.6 | 10.7 | 10.5 | 9.1 | **3.6** | - | | |
| ***A. wulfhaackei* SC3** | 0.2 | 13.3 | 7.2 | 10.4 | 9.6 | 10.1 | 10.3 | 11.8 | 1.0 | **4.3** | **3.7** | - | |
| ***A. wulfhaackei* SC4** | 0.4 | 14.1 | 5.9 | 9.4 | 8.7 | 8.4 | 10.0 | 10.5 | 9.9 | **4.0** | **3.4** | **3.7** | - |

the four mitochondrial genes (not shown here) show that the recovered topology is identical for each gene, without any discrepancies in the recovered nodes.

The addition of newly sequenced specimens from *A. wulfhaackei* subclade 2 (*Afroedura* sp. 6 *sensu* Branch et al. 2021) indicated the same general pattern as the other lineages, with some moderate genetic distances to the other *A. wulfhaackei* subclades as well as significantly higher genetic distances to any other Angolan *Afroedura* species (see Table 4). As the four *A. wulfhaackei* subclades show much lower inter-taxon distances to one another (< 5% in the partial *16S* gene; Table 4) than the average distance within recognised Angolan *Afroedura* species, this neither supports nor rejects the previous suggestion by Branch et al. (2021) to separate the identified candidate species around the central highlands (*Afroedura* sp. 5–7 *sensu* Branch et al. 2021) from the recently described *A. wulfhaackei*. The same is true for the previously discussed split of two identified subclades within the species *A. vazpintorum* (see Branch et al. 2021): the three genetically-divergent Bimbe specimens (NB 744–6) formed a separate clade with two new vouchers from Tchivinguiro (P0-97–8), while two new samples from Tundavala (P0-103–4) and one from Bimbe (NB 743) cluster with the lowland coastal subclade. Bimbe, Tchivinguiro and Tundavala are nearby sites situated in the southern highlands, on the edge of the Humpata plateau. Similar to the divergence within *A. wulfhaackei* subclades, the genetic divergence of the highland subclade from true *A. vazpintorum* is well below the 5% threshold identified here (Table 4). Nonetheless, since the average of the genetic differences for these candidate species clades is significantly lower than between the currently recognised *Afroedura* species in Angola, they are herewith pooled into their closest known species (*A. wulfhaackei* and *A vazpintorum*, respectively) for the SDM analyses and morphological comparisons, pending further research to verify their taxonomic status.

## Morphology

Results for the morphological comparisons are summarised in Table 5, and are discussed in more detail in the species descriptions below. The new material from Bocoio, Angola (*Afroedura* sp. 1) was similar to the central highland subgroup (*A. wulfhaackei* and *A. bogerti*) with regard to the lower numbers of scale rows on ventral and dorsal surface per tail verticil (4 and 5, respectively) and venter pigmented with fine black specks, but differed in that the supranasals were always in contact (similar to the south-western coastal sub-group comprising *A. donveae* and *A. vazpintorum*) versus separated by smaller granules (33% in *A. bogerti* and 57% in *A. wulfhaackei*) and higher number of precloacal pores (12 versus 8 in *A. bogerti* and 9.5 mean in *A. wulfhaackei* [although this might not be a true reflection as our male sample sizes of all species are limited]). The material from Otjihipa Mountains, northern Namibia (*Afroedura* sp. 2), conforms to the south-western coastal sub-group in the number of scale rows on ventral and dorsal surface per tail verticil (5 and 6, respectively), immaculate venter, bright dorsal colouration and boldly black-barred tail. It differs only in some minor scalation features and in that the iris is brown or copper-coloured (versus black in *A. donveae*).

## Species descriptions

Both genetics and morphology, as well as geographical separation, suggest that the *Afroedura* sp. 1 from Bocoio, Angola and *Afroedura* sp. 2 from Otjihipa, Namibia populations should both be regarded as new species. We apply the general lineage-based species concept, treating all populations that represent independent historical lineages supported by multiple different lines of evidence as separate species (de Queiroz 1998).

**Table 5.** Summary of morphological data for *Afroedura bogerti*, *A. wulfhaackei* (including members of the morphologically-indistinguishable subclades), *A. donveae*, *A. vazpintorum* (including isolated escarpment population), *A. praedicta*, *A. pundomontana* sp. nov. and *A. otjihipa* sp. nov. Values are given as a range with mean in parenthesis for scalation and mean ± standard deviation for meristic ratios. M = male, F = female, n = sample size.

| Character | *A. bogerti* | *A. wulfhaackei* | *A. donveae* | *A. vazpintorum* | *A. praedicta* | *A. pundomontana* sp. nov. | *A. otjihipa* sp. nov. |
|---|---|---|---|---|---|---|---|
| | (n = 9) | (n = 35) | (n = 17) | (n = 48) | (n = 5) | (n = 7) | (n = 2) |
| Snout vent length (maximum) | M 50 mm | M 60 mm | M 59.6 mm | M 58 mm | M 52 mm | M 58 mm | M 60 mm |
| | F 54 mm | F 59 mm | F 65 mm | F 59 mm | F 51 mm | F 58 mm | F 58 mm |
| Head Length/Head Width | 1.3 ± 0.09 | 1.4 ± 0.14 | 1.4 ± 0.08 | 1.3 ± 0.13 | 1.3 ± 0.14 | 1.3 ± 0.14 | 1.1 ± 0.12 |
| Snout Length/Eye Distance | 1.6 ± 0.34 | 2.0 ± 0.20 | 2.0 ± 0.19 | 1.8 ± 0.29 | 1.7 ± 0.19 | 2.0 ± 0.96 | 1.7 ± 0.12 |
| Snout Length/Eye-Ear Distance | 1.2 ± 0.07 | 1.2 ± 0.14 | 1.3 ± 0.30 | 1.2 ± 0.17 | 1.1 ± 0.09 | 1.2 ± 0.30 | 1.1 ± 0.06 |
| Precloacal pores (males only) | 8 (n = 1) | 9–11 (9.5) (n = 12) | 11–12 (11.5) (n = 4) | 9–11 (10.2) (n = 12) | 8 (8.0) (n = 3) | 12 (n = 1) | 12 (n = 1) |
| Ventral rows per tail verticil | 4 (4.0) | 4 (4.0) | 5–6 (5.5) | 5–7 (5.0) | 4 (4.0) | 4–5 (4.4) | 5 |
| Dorsal rows per tail verticil | 5 (5.0) | 5–6 (5.0) | 6–7 (6.6) | 6–7 (6.1) | 5 (5.0) | 5–6 (5.6) | 6 |
| Scales below 4th toe | 6–9 (6.9) | 6–9 (7.3) | 6–8 (7.7) | 6–10 (8.0) | 9–11 (9.6) | 7–9 (7.7) | 8 |
| Mid-body scale rows | 69–77 (73.5) | 73–88 (79.5) | 64–78 (72.8) | 73–86 (80.3) | 73–78 (74.8) | 78–82 (79.5) | 65–67 |
| Scales between eyes | 11–14 (12.4) | 11–16 (13.7) | 11–14 (11.0) | 11–15 (13.1) | 12–15 (13.5) | 13–15 (13.9) | 14 |
| Scales: nostril to eye | 8–12 (9.9) | 7–10 (8.3) | 8–11 (9.3) | 7–11 (9.1) | 9–10 (10.2) | 10–13 (10.9) | 10–11 |
| Scales: ear to eye | 14–16 (15.4) | 12–18 (15.90) | 11–14 (11.9) | 13–17 (15.6) | 13–16 (14.8) | 16–19 (16.9) | 12–13 |
| Supranasals in contact | 33% | 57% | 100% | 100% | 100% | 100% | 100% |
| Supralabials | 8–10 (8.4) | 7–9 (8.2) | 8–10 (9.0) | 8–10 (8.8) | 8–10 (9.2) | 8–9 (8.7) | 8–9 |
| Infralabials | 8–9 (8.3) | 8–9 (8.3) | 8–11 (9.3) | 8–9 (9.1) | 8–9 (8.5) | 9 (9.0) | 8–9 |

### *Afroedura pundomontana* sp. nov.

https://zoobank.org/556B8212-21E8-494A-BF1E-7B3021C53BA9

Bocoio Flat Gecko (English)

Osga-achatada do Bocoio (Portuguese)

Figs 3A–B, 4, 5C–D, Tables 5, 6

**Note.** According to Branch et al. (2021), historical material from near Bocoio in Benguela Province, Angola clustered morphologically with *A. wulfhaackei*. However, due to the occurrence at lower elevations and being isolated from other known populations of *Afroedura* it was suggested that the status of this population required further investigation (Branch et al. 2021). Newly-collected material allowed for its re-assessment within a wider phylogenetic framework, and it was determined that it represented a novel lineage, related to *A. bogerti* and not *A. wulfhaackei*, as initially hypothesised. It is therefore described below as a new species.

**Synonym.** *Afroedura bogerti* – Branch et al. 2017: 162; Marques et al. 2018: 178 (in part).

*Afroedura wulfhaackei* – Branch et al. 2021: 66 (in part).

**Holotype.** PEM R24743, adult female, collected at Morro do Pundo, about 25 km west of Bocoio (-12.44389, 13.92250; 946 m a.s.l.), Benguela Province, Angola by Pedro Vaz Pinto on 6 June 2018.

**Paratypes.** (six specimens). *TM 46587–8, TM 465890, adult females, collected 30 km W of Sousa Lara [= Bocoio] (approx. -12.40689, 13.90400; 670 m a.s.l.), Benguela Province, Angola by Wulf Haacke on 28 May 1974; *TM 46589, adult male, collected 30 km W of Sousa Lara [= Bocoio] (approx. -12.40689, 13.90400; 670 m a.s.l.), Benguela Province, Angola, by Wulf Haacke on 28 May 1974; FKH 0688, FKH 0689, adult females, collected from Alto Pundo – Bocoio (-12.44367, 13.92072, 920 m a.s.l.), Benguela Province, Angola by Pedro Vaz Pinto and Afonso Vaz Pinto on 2 September 2021. *Note the locality data presented as '3 km west of Bocoio, Benguela Province (12°28'58.0"S, 14°06'24.8"E)' in Branch et al. (2017, 2021) is in error and we update it according to the original specimen labels and catalogue museum register.

**Etymology.** The new species is named in reference to the area where it was found. The region lies on top of a ridge known as Morro do Pundo that translates to the 'Hills' or 'Mountain' of the Baboons. The name thus comprises two parts: *pundo* (= baboon) and *montana* (= mountain).

**Diagnosis.** A member of the greater *'transvaalica'* group, possessing two pairs of enlarged scansors per digit, and a strongly verticillate and flattened tail (Jacobsen et al. 2014). As part of the *A. bogerti* group it differs from other members of the *'transvaalica'* group by having 78–82 midbody scale rows (versus 97–102 in *A. gorongosa*, 113–120 in *A. loveridgei*, 102–119 in *A. transvaalica*); and rostral excluded from the nostril (in contact in *A. gorongosa*) [Note: in Branch et al. (2021) it was incorrectly recorded that the rostral is in contact with the nostril in the *A. bogerti*-group]; with the supranasals always being in contact (separated by 1–3 granules in *A. gorongosa*; always in broad contact in *A. loveridgei*; usually in broad contact in *A. transvaalica* ~ 3–18%); and in having 13–15 scales between the anterior borders of the eyes (19–22 in *A. gorongosa*; 15–19 in *A. loveridgei*; 15–20 in *A. transvaalica*) (comparative data *fide* Branch et al. 2017, 2021).

*Afroedura pundomontana* sp. nov. differs from other members of the *A. bogerti* group by a combination of the following characteristics (see Tables 5–6): midbody scale rows 78–82 (mean 79.5) (71–72 [mean 71.5] in *A. otjihipa* sp. nov., 65–67 [mean 66.0] in *A. donveae*, 69–77 [mean 73.5] in *A. bogerti*, 73–78 [mean 74.8] in *A. praedicta*, 73–88 [mean 79.5] in *A. wulfhaackei*, 73–86 [mean 80.3] in *A. vazpintorum*); by the supranasals always being in contact (~33% of the time in *A. bogerti*; ~57% in *A. wulfhaackei*; always in contact in *A. donveae*,

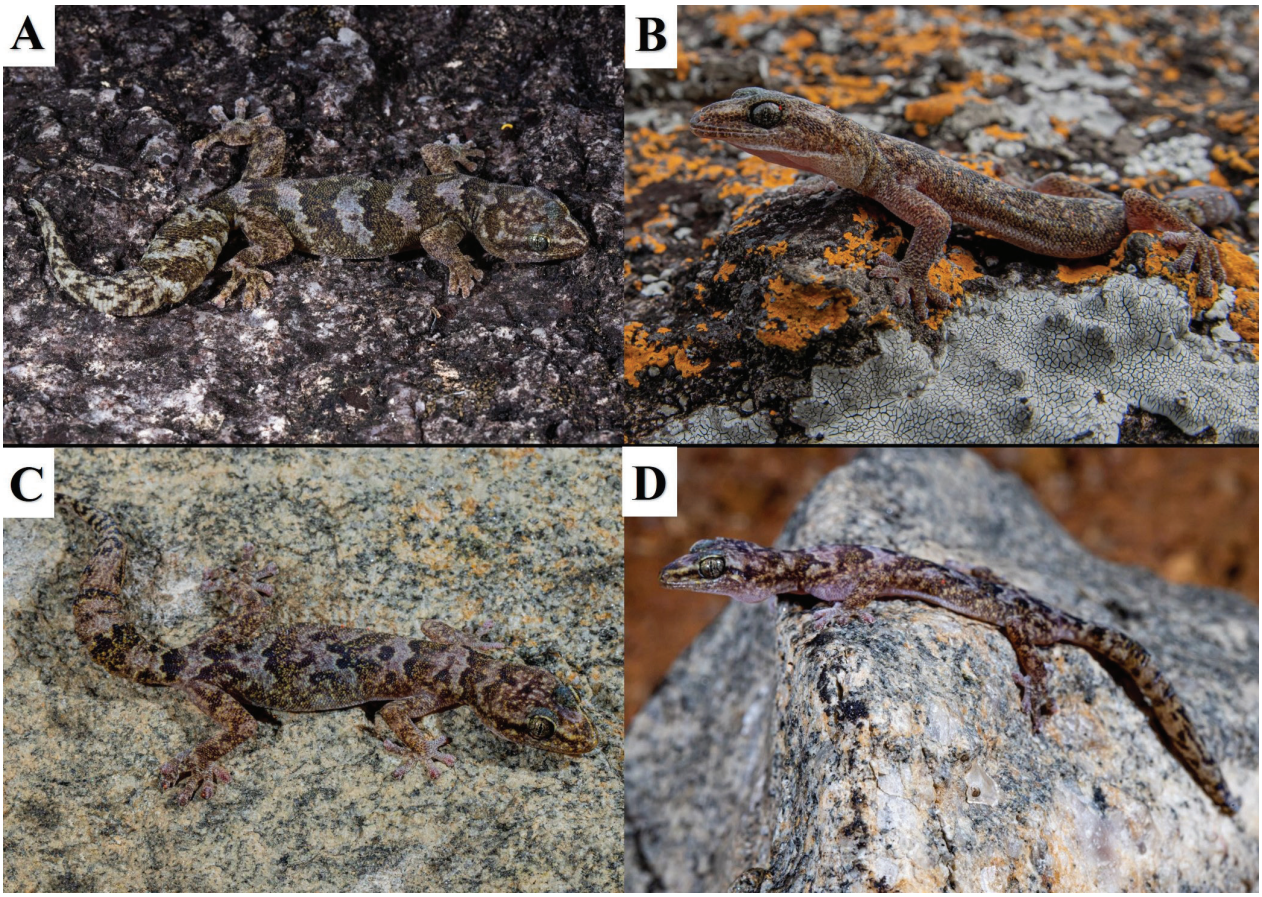


**Figure 3.** Live specimens of: **A–B.** *Afroedura bogerti* (**A.** P1-286, not vouchered; **B.** JLRZC0015, not vouchered) from Serra da Namba, Cuanza Sul Province, Angola; **C–D.** *Afroedura pundomontana* sp. nov. (FKH0689) from Morro do Pundo, Benguela Province, Angola. Photos: **A, C, D.** Pedro Vaz Pinto; **B**. Javier Lobón-Rovira.

*A. vazpintorum*, *A. praedicta* and *A. otjihipa* sp. nov.); each tail verticil comprising 4–5 (mean 4.4) ventral and 5–6 (mean 5.6) dorsal rows of scales (mean 4 ventral and 5 dorsal in *A. bogerti*, *A. praedicta* and *A. wulfhaackei*; 5–6 [mean 5.5] ventral and 6–7 [mean 6.6] dorsal in *A. donveae*; 5–6 [mean 5.0] ventral and 6–7 [mean 6.1] dorsal in *A. vazpintorum*; 5 ventral and 6 dorsal in *A. otjihipa* sp. nov.); ventral surfaces greyish with scattered small black spots (similar to *A. bogerti*, *A. praedicta* and *A. wulfhaackei*, immaculate in *A. donveae*, *A. vazpintorum* and *A. otjihipa* sp. nov.). *Afroedura pundomontana* sp. nov. differs from its sister highland species *A. bogerti* in having higher numbers of midbody scale counts (78–82 [mean 79.5] versus 73–78 [mean 74.8]), supranasals always in contact (versus ~33% of the time), and the posterior scales of the dorsal W-shapes crossbars dark black (versus same colour as cross bands; Fig. 3); it differs from *A. wulfhaackei* in that the supranasals are always in contact (versus ~57%).

**Holotype description.** Adult male; SVL 46.0 mm; tail 42.3 mm (detached full original tail). Small mid-ventral incision for removal of liver sample. Measurements and meristic characters of holotype are presented in Table 6. Head and body dorsoventrally compressed; HL 12.5 mm, HW 8.3 mm, broadest at posterior level of eye; head 1.51 times longer than wide. Eye large (2.6 mm wide), pupil vertical with indented margins; circumorbital scales small and smooth, elongate at upper anterior margin, upper three posterior scales with small upward pointing spines. Snout rounded, 4.9 mm long, longer than distance between eye and ear openings (3.8 mm). Scales on top of snout smooth, rounded; scales at the edge larger than central ones, with no intervening minute granules. Scales on snout slightly larger in size to those on the back of head or the nape. Scales on eyelids larger than those on the crown, six scales deep from circumorbital scale to crown. Circumorbital scales separated from the larger scales on the eyelids by two rows of smaller scales. Nostril pierced between first supralabial and three nasal scales; rostral excluded from nostril; 1st supralabial narrowly excluded from nostril; supranasal much larger than the postnasals (which are about equal in size) and in broad contact. Nostrils slightly elevated. Rostral roughly rectangular but with the upper edges slightly elongated due to extensions to the supranasals. Eight supralabials on either side, the labial margin flexing upwards at the rictus (approx. midorbital position), with 3–4 minute scales proximal to the flexure. Nine infralabials on either side, with a small scale proximal to the flexure. At the lip, mental slightly narrower than adjacent infralabial; mental only two thirds the width of rostral (1.1 mm versus 1.8 mm respectively), and in contact with three rounded postmental scales. Scales

**Figure 4.** Holotype of *Afroedura pundomontana* sp. nov. (PEM R24743) from Morro do Pundo, 25 km west of Bocoio, Benguela Province, Angola. Scale bar: 1 cm. Photos: Werner Conradie.

on throat notably smaller than those on belly, but the scales touching the infralabials are larger. Fourteen scales across the crown at level of front of eyes; 18 scales from ear to eye; 83 scales around midbody. Ear opening deep, oblique and more-or-less round, nearly symmetrical (0.7 × 0.8 mm). Scales on dorsum smooth, closely set but juxtaposed, largest at mid-body, smaller on nape and tail base. Scales on venter flattened, not overlapping, more-or-less ovate at mid-ventrum, about twice the size of lateral granules and about 1.5 times larger than the scales along the backbone. Original tail slightly dorsoventrally flattened and distinctly verticillate (10 distinct verticils in total), with obvious lateral constrictions that become less distinct towards the tip of the tail; each verticil comprising 6 rows of imbricate scales dorsally and 4 rows of imbricate ventrally, with ventral scales approximately twice the size of those on the dorsal surface. Limbs well-developed, hindlimbs slightly longer than forelimbs, no notable mite pockets (dermal crevices inhabited by small ectoparasitic mites) at anterior or posterior margin of hind limbs. All digits with a large pair of distal scansors, separated by a large, curved claw, and followed after a large gap (twice the length of terminal scansor) by a smaller pair of scansors; infero-median row of digital scales enlarged transversely, particularly towards the scansors, where the terminal scale adjoining the first pair of scansors may be medially constricted, swollen and scansor-like; seven enlarged subdigital lamellae on 4$^{th}$ toe.

**Paratype variation.** (see Table 6 for more measurements and scale counts of type series). SVL 43.4–57.8 mm; head length 1.19–1.50 times head width; snout 1.20–1.93 times the diameter of eye. Supranasals always in contact; the first upper labial and rostral always enter the nostril, and the width of the rostral at the lip margin is always wider than that of the mental; 2–3 postmental scales; supralabials 9, infralabials 9; scales between anterior edges of eyes 16–19; scales between nostril and anterior edge of orbit 10–13; scales between anterior edge of ear and rear margin of orbit 16–19; scales around midbody 78–83; subdigital lamellae of 4$^{th}$ toe 7–9; dorsal

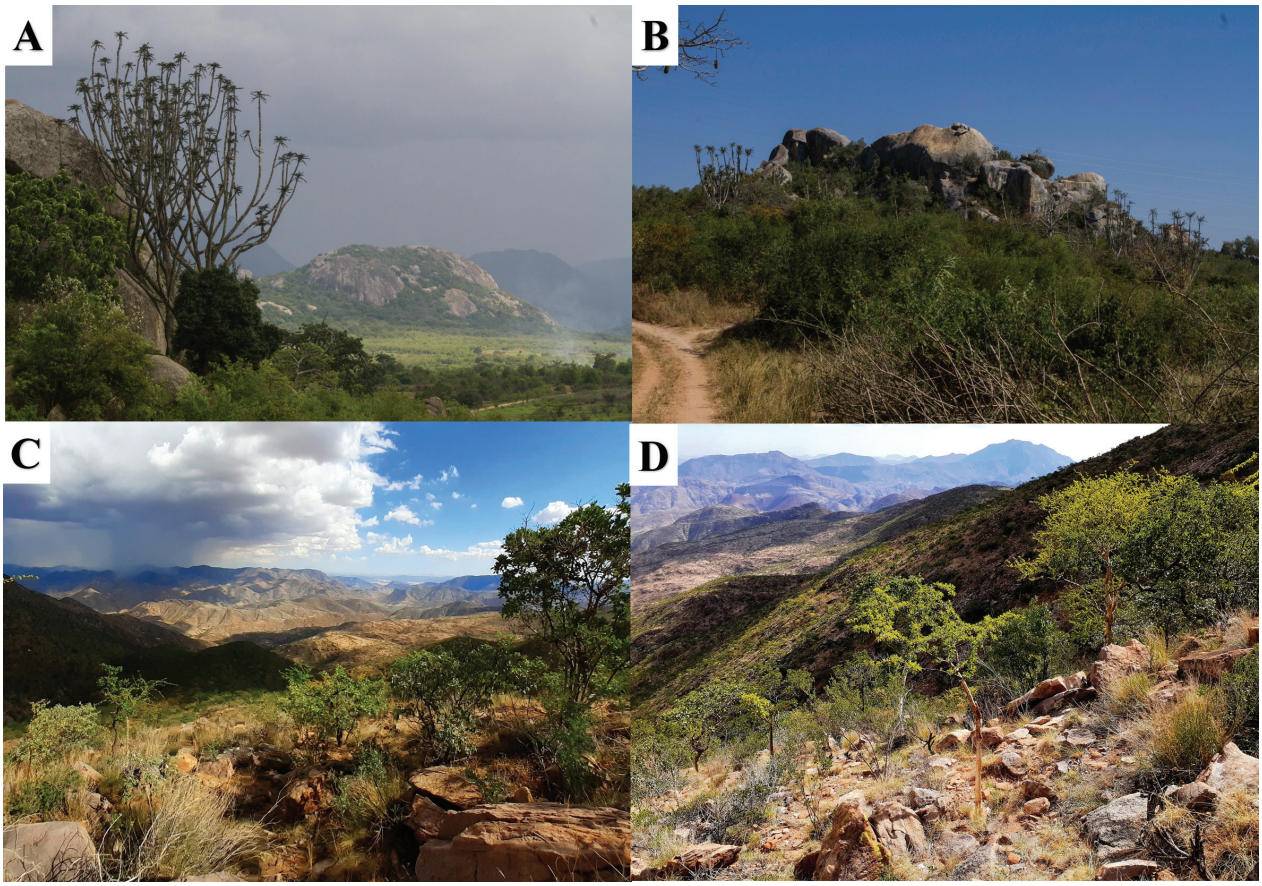


**Figure 5.** Habitat photos of: **A–B.** *Afroedura pundomontana* sp. nov.: Morro do Pundo, 25 km west of Bocoio, Benguela Province, Angola; **C–D.** *Afroedura otjipha* sp. nov.: Otjihipa Middleberg, Kunene Region, Namibia. Photos: **A–B.** Pedro Vaz Pinto; **C–D.** Francois Becker.

**Table 6.** Measurements (in mm) and scale counts for the type series of *Afroedura pundomontana* sp. nov.

| Catalogue Number | PEM R24743 | TM 46587 | TM 46588 | TM 46589 | TM 46590 | FKH0688 | FKH0689 |
|---|---|---|---|---|---|---|---|
| Type Status | Holotype | Paratype | Paratype | Paratype | Paratype | Paratype | Paratype |
| Sex | Female | Female | Female | Male | Female | Female | Female |
| Snout-vent length | 46.0 | 57.8 | 43.4 | 57.8 | 53.4 | 54.4 | 57.1 |
| Tail length | 42.3 | 61.5 | – | 44.1 | 47.33 | – | 47.1 |
| Tail condition | Original | Original | Truncated | Regenerated | Truncated | Truncated | Partly Regenerated |
| Head length | 12.5 | 13.0 | 10.6 | 13.3 | 12.7 | 13.1 | 15.0 |
| Head width | 8.3 | 10.3 | 8.3 | 11.2 | 10.1 | 10.6 | 11.9 |
| Snout length | 4.9 | 5.1 | 4.1 | 4.5 | 5.0 | 4.6 | 4.8 |
| Eye distance | 2.6 | 3.5 | 3.1 | 3.7 | 4.0 | 2.6 | 2.5 |
| Eye-Ear distance | 3.8 | 4.5 | 3.5 | 4.7 | 3.7 | 4.4 | 4.3 |
| Precloacal pores (males) | – | – | – | 12 | – | – | – |
| Dorsal rows per tail verticil | 4 | 4 | 5 | – | 4 | – | 5 |
| Ventral rows per tail verticil | 6 | 5 | 6 | – | 5 | – | 6 |
| Scales below 4$^{th}$ toe | 7 | 8 | 9 | 8 | 8 | 7 | 7 |
| Midbody scale rows | 83 | 81 | 78 | 82 | 78 | 78 | 80 |
| Scales between eyes | 14 | 14 | 13 | 13 | 13 | 15 | 15 |
| Scales: nostril to eye | 11 | 10 | 10 | 10 | 11 | 12 | 13 |
| Scales: ear to eye | 18 | 15 | 16 | 16 | 16 | 19 | 18 |
| Supranasals in contact | Yes | Yes | Yes | Yes | Yes | Yes | Yes |
| Supralabials | 8 | ? | ? | ? | ? | 9 | 9 |
| Infralabials | 9 | ? | ? | ? | ? | 9 | 9 |

scale rows per tail verticil 5–6; ventral scale rows per tail verticil 4–5. Precloacal pores 12 (single male).

**Colouration.** ***In life*** (holotype PEM R24743 [similar to Fig. 3C–D]): Greyish above with five evenly spaced darker crossbars from the occiput to the sacrum, each crossbar consisting of 9–12 dark scales forming a distinct W-shape, that consist anteriorly of a mix of grey and mustard scales and posteriorly by more prominent dark grey to black scales; each dark crossbar is separated by a mix of lighter grey scales; head with irregular dark grey blotches on the crown with intervening pale grey and mustard colouration; dark grey bar from nostril to the anterior margin

of the ear opening; a vague, thin grey canthal stripe, extends on both sides from the nasal region to anterior margins of eye; upper and lower labials light grey anteriorly and beige posteriorly with fine black specks; lateral sides of the body with a mix of light grey and light cream-yellow; limbs light greyish above with scattered darker grey markings interspersed with cream-yellow; tail with eight dark brown to black crossbands, becoming increasingly more bold towards the tip; iris gold in colour with a narrow black elliptic pupil with crenulated edge, and black reticulation with light grey intervening blotches; venter uniform greyish with scattered black specks; ventral part of limbs with scattered black specks, more prominent than on the underparts. ***In preservative*** (Fig. 4): Dorsum with five evenly spaced dark brown W-shaped crossbars from the occiput to the sacrum with beige intervening blotches; ventrum is beige with numerous small scattered black specks on each scale, more prominent posteriorly; tail with eight dark brown to black cross bands. ***Paratype colouration variation***: greyish above with five to six evenly or irregularly spaced darker grey-black W-shaped crossbars from the occiput to the sacrum, anterior part of these crossbars much darker than the posterior part, which is scattered with mustard coloured scales; lateral sides of body with a mixture of darker grey and mustard coloured scales; limbs and tail with grey blotches, with scattered mustard coloured scales; ventrum uniform greyish with scattered black specks.

**Natural history and habitat.** (Fig. 5A–B). A rupicolous species found in rugged landscape between 600 to 1,000 m a.s.l. No details are available regarding the conditions under which the historical material was collected, but the new material was collected during the day, underneath vertical flakes in large granite boulders. On both occasions, several individuals were sheltering under the same flake. They were found in rocky outcrops in anthropogenically disturbed mixed escarpment woodland, characteristic of the ecotone between the arid coastal plain and the inland mesic Angolan plateau. The presence of shrubs and small trees surrounding the granite outcrops suggests that these geckos might forage at night in the vegetation as reported for other Angolan species (Branch et al. 2021).

**Distribution and conservation.** This species is currently known only from central Benguela Province, Angola (Fig. 2). It was collected at three localities in close proximity to one another, on the first elevation step of the Angolan escarpment, inland from the town of Lobito. The species may be more widely distributed as our predicted mapping indicates but, so far, surveys conducted on the coastal plain and elsewhere along the escarpment did not produce additional material. Even around the type locality, the species proved to be uncommon and quite difficult to find, partly due to the inaccessible topography, but apparently also due to scarcity of granite flakes. Populations in isolated granite outcrops may be threatened by removal of rock flakes for construction of homes and other buildings. In accordance with IUCN Red List Guidelines (IUCN 2022) we propose this species to be classified as Data Deficient (DD) at this stage.

### *Afroedura otjihipa* sp. nov.

https://zoobank.org/B3818B24-7FF0-49B6-B6F9-F580BF50C0C0

Otjihipa Flat Gecko (English)

Otjihipa Platgeitjie (Afrikaans)

Figs 5C–D, 6C–D, 7, Tables 5, 7

**Synonym.** *Afroedura* cf. *bogerti* – Branch 1998: 232; Griffin 2002: 20, 2003:10; Herrman and Branch 2013: 5.

**Holotype.** NMNW R11253, adult female, collected from Otjihipa Middleberg (-17.28314, 12.66506, 1,900 m a.s.l.), Kunene Region, Namibia, by Morgan Hauptfleisch, Francois Becker, Vera De Cauwer, Wessel Swanepoel and Ernst van Jaarsveld on 23 April 2021.

**Paratype.** NMNW R11245, adult male (paired with female NMNW R11253 in same rock crack). Same collection details as holotype.

**Etymology.** The new species is named in reference to the area it was collected, namely Otjihipa Mountains in northern Namibia.

**Diagnosis.** A member of the greater '*transvaalica*' group as it possesses two pairs of enlarged scansors per digit and a strongly verticillate and flattened tail (Jacobsen et al. 2014). Part of the *A. bogerti* group which differs from other members of the '*transvaalica*' group by having less than 72 mid-body scale rows (vs. 97–102 in *A. gorongosa*, 113–120 in *A. loveridgei*, 102–119 in *A. transvaalica*); rostral excluded from the nostril (in contact in *A. gorongosa*); supranasals always in contact (separated by 1–3 granules in *A. gorongosa*; always in broad contact in *A. loveridgei*; usually in broad contact in *A. transvaalica* ~ 3–18%); and 15–16 scales between anterior borders of the eyes (19–22 in *A. gorongosa*, 15–19 in *A. loveridgei*, 15–20 in *A. transvaalica*) (comparative data from Branch et al. 2017, 2021).

*Afroedura otjihipa* sp. nov. differs from other members of the *A. bogerti* group by a combination of the following characteristics (see Tables 5 and 7): 65–67 (mean 66.0) mid-body scale rows (64–78 [mean 72.8] in *A. donveae*, 69–77 [mean 73.5] in *A. bogerti*, 73–78 [mean 74.8] in *A. praedicta*, 78–82 (mean 79.5) in *A. pundomontana* sp. nov.; 76–88 [mean 79.3] in *A. wulfhaackei*, 73–86 [mean 80.3] in *A. vazpintorum*); supranasals always in contact (similar to *A. donveae*, *A. vazpintorum*, *A. praedicta* and *A. pundomontana* sp. nov.; in contact in ~ 33% of *A. bogerti*; in contact in ~ 57% *of A. wulfhaackei*); each tail verticil comprises 5 ventral and 6 dorsal rows of scales (mean 4 ventral and 5 dorsal in *A. bogerti*, *A. praedicta* and *A. wulfhaackei*; 4–5 (mean 4.4) ventral and 5–6 (mean 5.6) dorsal in *A. pundomontana* sp. nov.; 5–6 [mean 5.5] ventral and 6–7 [mean 6.6] dorsal in *A. donveae*; 5–6 [mean 5.0] ventral and 6–7 [mean 6.1] dorsal *A. vazpintorum*); ventral surfaces light cream and almost immaculate, with some scattered dark spots near lateral edges (similar to *A. donveae* and *A. vazpintorum*; greyish

**Table 7.** Measurements (in mm) and scale counts for the type series of *Afroedura otjihipa* sp. nov.

| Catalogue Number | NMNW R11253 | NMNW R11245 |
|---|---|---|
| Type Status | Holotype | Paratype |
| Sex | Female | Male |
| Snout-vent length | 57.9 | 59.9 |
| Tail length | – | – |
| Tail condition | Truncated | Regenerated |
| Head length | 13.6 | 15.9 |
| Head width | 13.2 | 13.3 |
| Snout length | 5.7 | 6.0 |
| Eye distance | 3.2 | 3.8 |
| Eye-Ear distance | 4.8 | 5.4 |
| Precloacal pores (males) | – | 12 |
| Dorsal rows per tail verticil | 5 | 5 |
| Ventral rows per tail verticil | 6 | 6 |
| Scales below 4th toe | 8 | 8 |
| Midbody scale rows | 67 | 65 |
| Scales between eyes | 14 | 14 |
| Scales: nostril to eye | 10 | 11 |
| Scales: ear to eye | 12 | 13 |
| Supranasals in contact | Yes | Yes |
| Supralabials | 8 | 9 |
| Infralabials | 9 | 8 |

with black spots in *A. bogerti, A. wulfhaackei*, *A. praedicta* and *A. pundomontana* sp. nov.); larger average adult size 58.2 mm SVL (versus 57.6 mm in *A. donveae*, 51.7 mm in *A. wulfhaackei*, 51.3 mm in *A. vazpintorum*; 50.3 mm in *A. pundomontana* sp. nov., 50.0 mm in *A. bogerti*, 49.9 mm *A. praedicta*), and by having very distinct black-and-white tail banding (similar to *A. donveae*). *Afroedura otjihipa* sp. nov. differs from its sister lowland species *A. donveae* in having a brown or copper coloured (versus black) iris, a relatively broader head (mean HL/HW 1.1 versus 1.3), and in dorsal colour pattern (Fig. 6): in *A. otjihipa* sp. nov. it is dominantly dark brown, the yellow appearing as small asymmetrical, irregular patches, and as irregular borders of four paired, asymmetrical, irregular, roughly triangular brown blotches, which merge at the scapular and sacral regions to form two additional bands (versus roughly symmetrical brown patterns on a mostly yellow background in *A. donveae*).

**Holotype description.** Adult female: SVL 57.9 mm; tail regenerated, with a small mid-ventral incision for the removal of liver sample. Measurements and meristic characters of holotype presented in Table 7. Head and body dorsoventrally depressed; HL 13.6 mm, HW 13.2 mm, head broadest posterior level of eye and 1.02 times longer than wide. Eyes large (3.2 mm wide), pupil vertical with indented margins; circumorbital scales small and smooth, bottom posterior scales with small upward pointing spines. Snout rounded, 5.7 mm long, longer than distance between eye and ear openings (4.8 mm). Scales on top of snout smooth, rounded, similar in size, with no intervening minute granules. Scales on snout slightly larger than those on back of head or nape. Scales on eyelids larger than those on the crown, 5 scales deep from circumorbital scale to crown. Nostril pierced between first supralabial and three nasal scales; rostral narrowly excluded from nostril; supranasals much larger than the smaller postnasals, ventral postnasal being about half the size of its dorsal counterpart, and all in broad contact with one other. Nostrils very slightly elevated. Rostral roughly rectangular, but with its upper edges elongated due to extensions toward the nostril, and the central point extends between the nasals. Seven supralabials on each side, the labial margin flexing upwards at the rictus (approx. mid-orbital position), with 1–2 elongate scales proximal to the flexure and several minute scales along the flexure proximal to these. Seven infralabials on either side. At the lip, mental scale slightly narrower than adjacent infralabial, mental only two thirds the width of rostral (1.1 mm versus 1.8 mm respectively) and in contact with three postmental scales; mental similar in size and shape to the surrounding gular scales, the central one of which is distinctly smaller. Scales on throat much smaller than those on belly, scales touching infralabials larger. Fourteen scales across the crown at level of front of eyes; 10 scales between nostril and front of eye; 12 scales from ear to eye; 67 scales around mid-body. Ear opening deep, oblique and roughly oval, less than half as high as wide (0.42 × 0.95 mm respectively). Scales on dorsum smooth, non-overlapping, largest at mid-body, smaller on nape and tail base. Scales on ventrum flattened, not overlapping, roughly twice the size of lateral granules and 1.4 times the size of scales along the dorsal mid-line. Regenerated tail dorsoventrally flattened, roughly as broad as the neck, with ventral scales larger than those on the dorsal surface. Limbs well-developed, hindlimbs slightly longer than forelimbs; all limbs without obvious mite pockets at posterior or anterior margin of limb insertions. All digits with a large pair of distal scansors, separated by a curved claw, notably smaller on the fingers than toes, and followed after a gap (about the width of terminal scansor) by a smaller pair of scansors; infero-median row of digital scales slightly enlarged transversely, the distal two rows being paired in both digits and toes, where the terminal scale adjoining the first pair of scansors may be swollen and scansor-like; 6 enlarged central and two paired distal scale rows under 3rd toe, while other toes have paired scale rows, 8 under the 4th toe.

**Paratype variation.** SVL 59.9 mm adult male, tail truncated, precloacal pores 12. Measurements and meristic characters of paratype are presented in Table 7. The paratype is very similar to the holotype with regard to scalation.

**Colouration.** ***In life*** (holotype NMNW R11253, Fig. 7C–D): dark brown with yellowish patterns, fading to whitish on limbs and top of head; yellow patterns are irregular, asymmetrical patches and spots along the body, symmetrical paired spots around the nape and near the tail base; there is a thin, irregular, broken or continuous yellow bar on the nape; another broken, irregular yellow bar across the scapular region to the shoulders; three asymmetrical yellow double-bars which may present as pairs of medially-angled triangles posteriorly, across the back, each with an irregular dark brown core; another broken yellow bar or collection of symmetrical spots around the sacrum; head dark brown with yellow blotches

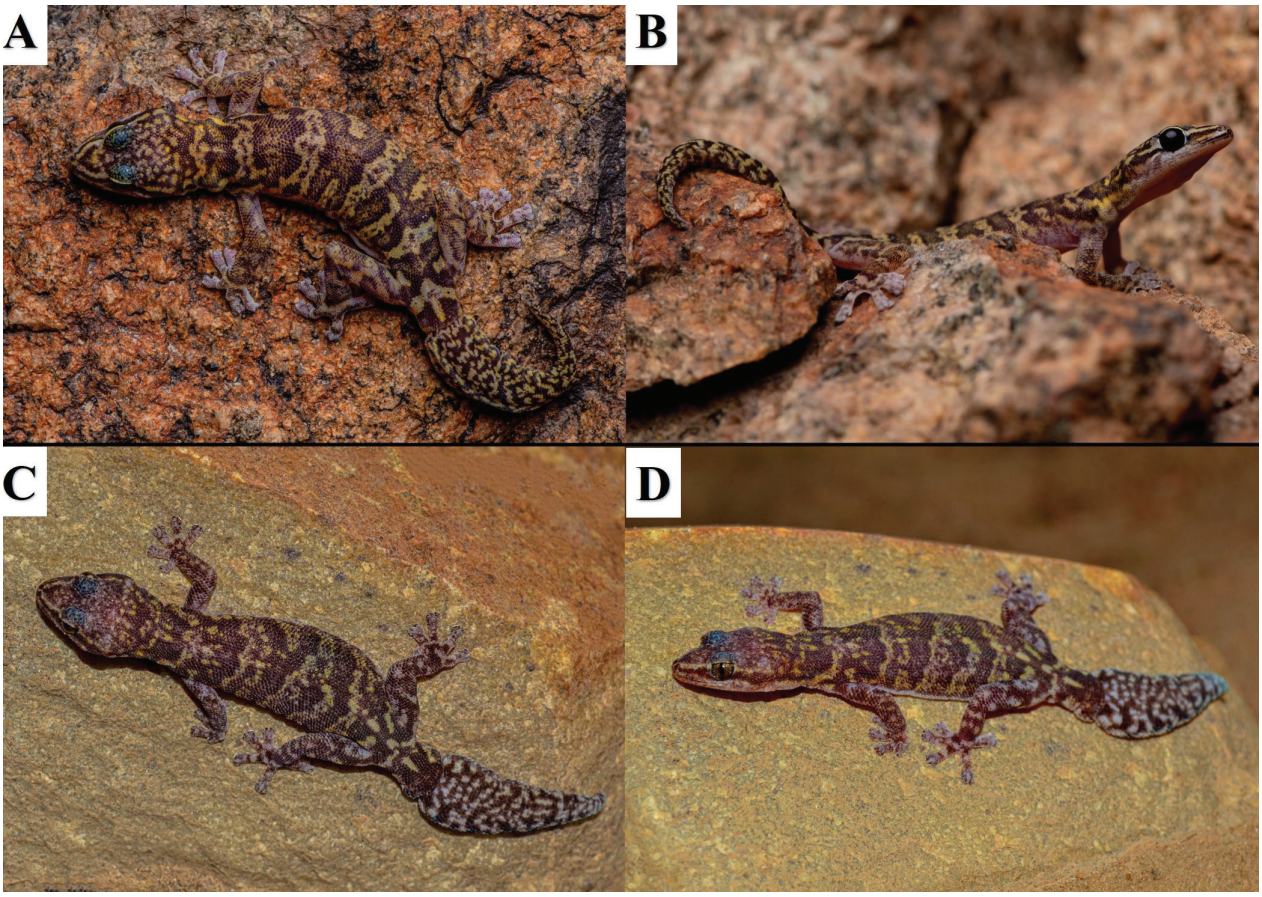


**Figure 6.** Live specimens of: **A–B.** *Afroedura donveae* from Omahua, Namibe Province, Angola (not sampled); **C–D.** *Afroedura otjihipa* sp. nov. (holotype female, NMNW R11253) from Otjihipa Middleberg, Kunene Region, Namibia. Photos: **A–B.** Javier Lobón-Rovira; **C–D**. Francois Becker.

on the crown with intervening pale yellow colouration; dark brown bar from nostril across the upper margins of the ear opening, connecting with dark brown lateral bar on the neck; a thin pale yellow canthal stripe extends on both sides from the nasal region to anterior margins of eye, continuing posteriorly from the eye onto the nape; skin above eyes copper blue with dark brown spots; upper and lower labials light grey with dense brown speckling, denser anteriorly and on supralabials; lateral sides of the body with a mix of dark brown and yellowish blotches, as a continuation of the dorsal patterns; limbs dark brown above with scattered light grey markings; tail (regenerated) with an asymmetrical chequered pattern of dark brown and light grey; iris copper in colour with a narrow black elliptic pupil with crenulated edge, and black reticulation; venter uniform beige with scattered brown specks mostly on lateral edges; ventrally, limbs with scattered brown spots, mostly near lateral surfaces. In preservative: yellowish patterns faded to light grey, dark brown to grey-brown, and eyes faded to bluish grey, with original colouration of pupils and iris no longer evident. ***Paratype colouration***: Similar colouration and patterning as to the holotype, but the yellow bands and patterns are more clearly defined: the bar on the nape is nearly continuous, that on the scapular region has a clear dark brown core, and three pairs of asymmetrical, medially-pointing, dark brown, triangular blobs are clearly outlined by irregular yellow lines; no clear bar near the tail base, but a collection of symmetrical spots. The original tails are not present on the preserved specimen, but were observed briefly in life before capture. The original tails of another pair of individuals in a nearby rock crack (not caught) were also observed. Tail bars could not be counted, but bold black-and-white banding was clearly visible.

**Natural history and habitat.** A rupicolous species living in narrow rock crevices in relatively small sandstone outcrops in arid woodland savannah (Fig. 5C–D), at elevations of 1,800–1,900 m a.s.l. in the Otjihipa Mountains. It was not found in the dolomite formations near the type locality, despite greater search time dedicated to those areas. The rock cracks where they were found were smaller than is typical for this group and were similar throughout this surface formation. Congeners in the *A. bogerti* group are normally found only in deep rock cracks in and amongst large boulders. Such habitat features were present in the surveyed area, but only in dolomite formations. The much less crevice-rich sandstone formation, with thin, straight cracks formed between the sandstone strata, appeared to be favoured syntopically by *A. otjihipa* sp. nov. and *Cordylus namakuiyus*.

**Distribution and conservation.** Currently known from a single sandstone ridge on Otjihipa Middleberg in

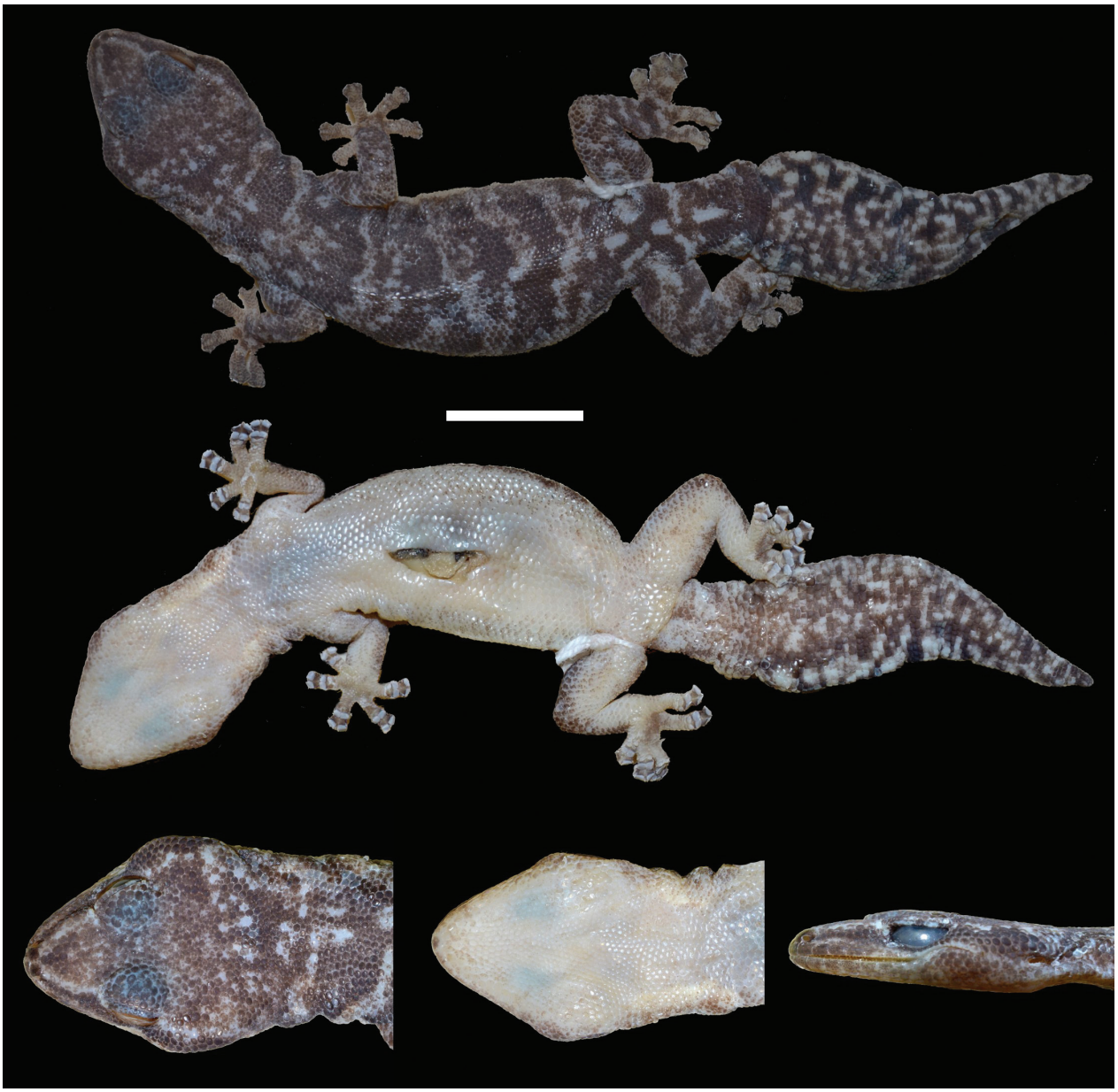

**Figure 7.** Holotype of *Afroedura otjihipa* sp. nov. (NMNW R11253) from Otjihipa Middleberg, Kunene Region, Namibia. Scale bar: 1 cm. Photos: Francois Becker.

the extreme north-west of the Kunene Region, Namibia (Fig. 2). The species remains poorly known, but it is probably stable in numbers as the local habitat is currently not threatened and is topographically unsuitable for human habitation. It likely occurs more broadly across the Otjihipa Mountain range. In accordance with IUCN Red List Guidelines (IUCN 2022) we propose this species to be classified as Data Deficient (DD) at this stage, but due to the remoteness of the locality and because no notifiable threats exist, it could be listed as Least Concern.

## Updated key to the *Afroedura bogerti*-group (updated from Branch et al. 2021)

1 Midbody scale rows more than 95 ..... 2
– Midbody scale rows less than 95; occurs in northern Namibia and Angola ..... 4
2 Rostral usually bordering nostril ..... 3
– Rostral usually excluded from nostril ..... *A. loveridgei*
3 Anterior nasals in contact (very rarely separated); scales around midbody: South Africa 102–118 (mean 109), northern Zimbabwe 108–119 (average 114) ..... *A. transvaalica*
– Anterior nasals separated by 1–3 granules; scales around midbody 99–101 (average 100) ..... *A. gorongosa*

4 Each tail verticil usually comprising 5 ventral and 6 dorsal rows of scales; anterior nasals always in contact; ventrum immaculate ..... 5
– Each tail verticil usually comprising 4 ventral and 5 dorsal rows of scales; anterior nasals not always in contact; ventrum greyish with small black specks ..... 6
5 Midbody scales 78–82 (mean 79.5) larger average adult size 57.1 mm SVL; precloacal pores 11–12 (mean 11.5) in males; bold colouration, black iris, occurs in Angola ..... *A. donveae*
– Midbody scales 65–67; larger average adult size 59.9 mm SVL; precloacal pores 12 in males; bold colouration, golden iris, occurs in Namibia ..... *A. otjihipa* sp. nov.
– Midbody scales 73–86 (mean 80.3); smaller average adult size 48.6 mm SVL; precloacal pores 9–11 (mean 10.2) in males; dull colouration ..... *A. vazpintorum*
6 Anterior nasals always in contact, restricted to first elevation step and isolated inselbergs below the Angolan escarpment ..... 7
– Anterior nasals not always in contact, restricted to above the Angolan escarpment ..... 8
7 Restricted to Serra de Neve Mountains, Namibe Province ..... *A. praedicta*
– Occurs on the first elevation step of the Angolan escarpment, Benguela Province ..... *A. pundomontana* sp. nov.
8 Midbody scales 69–77 (mean 73.5) ..... *A. bogerti*
– Midbody scales 76–88 (mean 79.3) ..... *A. wulfhaackei*

# Discussion

The addition of newly collected material from northern Namibia and western Angola, as well as the inclusion of more genes, improved the phylogenetic support values and relationships between species. The topology recovered remained very similar to those found in Branch et al. (2017, 2021), except this study resulted in the addition of two novel lineages here described as new species: *A. pundomontana* sp. nov. and *A. otjihipa* sp. nov. To avoid a potential overestimation of the number of taxa in a dataset, we took a conservative approach, recognising only those lineages where consistent morphological differences were evident and where genetic differences exceeded 5% in the *16S* gene as representing valid species. Deep genetic sub-structuring persists within *A. wulfhaackei* and *A. vazpintorum* and it will require finer-scale genetics to resolve their taxonomic status.

*Afroedura* is a genus of flat geckos that is restricted to rocky and mountainous habitat and inhabits both the eastern and western southern Africa escarpments, while the central Kalahari and Zambezi basin regions (generally fluvial lowlands and few or no mountains or inselbergs) appear to be devoid of these flat geckos (Branch 1998; Jacobsen et al. 2014). However, there are surprising links between the eastern and western populations, with *A. transvaalica*, *A. loveridgei* and *A. gorongosa* from eastern Zimbabwe and adjacent Mozambique highlands being sister species to the *A. bogerti*-group in western Angola and adjacent Namibia (Jacobsen et al. 2014; Branch et al. 2017, 2021). Preliminary dating analyses (results not shown here) suggest that the initial split between the two main *A. bogerti* lineages (*praedicta* + *otjihipa* + *donveae* + *vazpintorum* and *pundomontana* + *bogerti* + *wulfhaackei*) occurred between the late Pliocene and early Pleistocene, thus suggesting that rocky habitats throughout the southern inland parts of Africa may have, historically, been connected between eastern and western extremes. These preliminary dating findings still need to be confirmed in future studies which utilise all known species of the genus *Afroedura*.

The *Afroedura bogerti*-group is endemic to the central highlands and south-west coastal regions of Angola, with one species endemic to the Otjihipa Mountains, south of the Kunene River, in the northern Kunene region of Namibia. This group does not extend further south into the Namibian portion of the western escarpment. The only other species of *Afroedura* known to occur intermittently along the highlands of Namibia are taxa in the *A. africana*-group, which are closely related to South African species, and *A. tirasensis*, the phylogenetic relationship of which is still unknown (Jacobsen et al. 2014).

Our results show that the *Afroedura bogerti*-group speciation is driven by the complex landscape mosaic of rocky/mountainous and flat lowland habitats, under the influence of the steep climatic gradient characteristic of the Angolan escarpment region and exacerbated by Pleistocene climatic events. The basal split in the group is between the clade inhabiting higher rainfall mountains in the north-eastern extreme of its range (*A. bogerti*, *A. pundomontana* sp. nov. and *A. wulfhaackei*), and the clade inhabiting the predominantly more arid coastal regions in the southwest (*A. donveae*, *A. praedicta*, *A. otjihipa* sp. nov. and *A. vazpintorum*). This could be associated by a major ecological landscape transformation, such as with the expansion of $C_4$ grasslands, which occurred in the period between 2.0 and 1.75 Mya, and which has led to strong evolutionary pressure and species turnover in other African fauna (Bibi and Kiessling 2015).

The basal split within the inland highland lineages (*A. bogerti* + *A. wulfhaackei* + *A. pundomontana* sp. nov.) is between the strictly higher-lying inland species (*A. wulfhaackei*) and the subgroup formed by *A. bogerti* + *A. pundomontana* sp. nov. The latter subgroup further split into northern (*A. bogerti*) and western (*A. pundomontana* sp. nov.), lineages, currently present on an isolated mountain to the north and on the intermediate elevational step of the central escarpment, respectively. Although nomi-

notypical *A. bogerti* is currently only known to occur at Namba Mountain, and is geographically and ecologically closer to some populations of *A. wulfhaackei*, the genetic results suggest a past link maintained along the Angolan western escarpment. Namba Mountain is unique in containing more extensive forested habitats than any other Angolan highland, and clear phylogenetic relationships between Namba and the western escarpment have been revealed in various faunistic groups, such as rupicolous dwarf toads of the genus *Poyntonophrynus* (Baptista et al. in prep.). More recently, several *A. wulfhaackei* populations may have become isolated on scattered mountain tops or granitic outcrops in the central highlands, leading to the evolution of the four subclades already identified. This study suggests that these subclades are a consequence of an ongoing incipient speciation process. Moreover, the habitat, ecological niche and morphological conservatism, seem to be consistent with non-adaptive radiation, similar to what has been reported for other reptile radiations (e.g. Reaney et al. 2018).

On the other hand, the south-western lineages (*A. donveae* + *A. praedicta* + *A. otjihipa* sp. nov. + *A. vazpintorum*) have a more complex history of contraction, recolonisation and secondary contact, probably due to climatic changes exerted on a dynamic and highly heterogeneous landscape. The former three species seem very localised in their distributions, with high levels of specialisation. *Afroedura praedicta* and *A. otjihipa* sp. nov. are present only on two inselbergs separated by over 400 km of arid lowlands, contrasting with *A. donveae*, which occurs in the Angolan Kaokoveld desert and is the only species within the southwestern lineages, exclusively found in lowlands. While *A. donveae* and *A. praedicta* are associated with isolated large granite boulders, *A. otjihipa* sp. nov. lives among small rocks and vegetation. This suggests that the speciation of this group was likely caused by vicariance following the severe contraction of a once widespread ancestral taxon. Geographically intermediate populations between northern *A. praedicta* and southern *A. donveae* likely disappeared in response to extreme climatic and habitat changes, creating a large unoccupied area in between, while *A. otjihipa* sp. nov. may reflect a relatively recent colonisation (see Fig. 2). A deep split has been revealed within *A. vazpintorum*, leading to two subclades, and contemporaneous with the separation between *A. praedicta* and *A. donveae* + *A. otjihipa* sp. nov., when extreme environmental conditions may have forced various *Afroedura* populations to become isolated on mountain tops. Pinpointing the geographical origins of both subclades may not be possible, but their geographical distribution, together with the molecular results, suggest that when environmental conditions became suitable, *A. vazpintorum* expanded its range and populated the lowlands, eventually becoming the only widespread lineage within the genus. Although we lack occurrence records connecting coastal and inland subclades of *A. vazpintorum* populations, secondary contact is demonstrated by the presence of mitochondrial introgression of the coastal subclade in two of the three southern highland sites surveyed, including at Bimbe. The relationships between the coastal and inland lineages of *A. vazpintorum* need further investigation by using more informative nuclear markers, and an increased survey effort at the base of the southern escarpment, to test for current gene flow isolation.

Although the southwestern regions of Angola include some dramatic and heterogeneous topographic features and may have experienced geomorphological transformation throughout the Pleistocene, such as the gradual escarpment uplift (Feio 1981), it is likely that speciation in Angolan *Afroedura* was driven mostly by climatic factors. Our preliminary dating estimates seem to indicate that most node splits within the *A. bogerti* complex seem to have occurred in the Mid-Pleistocene Transition, a period when the change in orbital cycles led to shifts towards increasingly variable and drier climate in Africa, consequently promoting a speciation pulse (deMenocal 2004). All remaining splits recovered in our study, originating with *A. donveae* and *A. otjihipa* sp. nov. and leading to the diversification into subclades within *A. wulfhaackei*, must be of much younger origin but have very likely also resulted from strong environmental pressure. These diversification episodes could have been driven by glacial cycles, but linking each node split to specific climatic events will probably remain impossible.

Many species occur in largely undisturbed remote areas with little human interference or development, and populations can therefore be considered stable. However, most species are range-restricted, and future developments could quickly change their conservation status. A steep climatic gradient influenced by a steep-sloped, west-falling escarpment and the influence of the Atlantic Ocean, may render these specialised and topographically-isolated, high-altitude habitats particularly sensitive to climate change. The impacts of climate change on species endemic to high elevation have been found to be disproportionately high (Dirnböck et al. 2011). Therefore, surveys to monitor population size and determine population trends over time as associated with climatic changes, are a priority for the range-restricted species. Additional exploratory surveys to improve the accuracy of projected species ranges, particularly in the poorly-sampled Namibian Kaokoveld, are also needed.

## Acknowledgements

We thank Instituto Nacional da Biodiversidade e Conservação (INBC) of the Ministry of Culture, Tourism and Environment (MCTE, Luanda, Angola), and especially the director of INBC, Dr Albertina Nzuzi, for issuing research export permits. We also thank Fernanda Lages and Vladimir Russo for co-ordinating institutional relationships and facilitating work authorisations, and Afonso Vaz Pinto for collecting efforts at Bocoio. We acknowledge the important role played by Rolf Becker, Ansie Bosman, Wessel

Swanepoel and Vera De Cauwer in conceiving and organising the helicopter mountain-top surveys in Namibia and southern Angola, and Fernanda Lage and Vladimir Russo for co-ordinating institutional relationships and facilitating work authorisations in this regard. The SCIONA - Biodiversity Survey of Mountain Tops in the Kaokoveld Centre of Endemism was done in partnership with the Ministry of Culture, Tourism and Environment of the Republic of Angola and the Ministry of Environment, Forestry and Tourism of Namibia, and was funded by the European Union under grant agreement FED/2017/394-802. We thank Chad Keates for the generation of additional genes for newly collected material from northern Namibia, through the use of infrastructure and equipment provided by the NRF-SAIAB Aquatic Genomics Research Platform.. JLR were supported by Fundação para a Ciência e Tecnologia (FCT) and BIOPOLIS (PD/BD/140808/2018 and BIOPOLIS 2022-18, respectively). We thank Lemmy Mashini and Adriaan Jordaan for access to material housed in the Ditsong National Museum of Natural History (Pretoria, South Africa). This work was supported by the European Union's Horizon 2020 Research and Innovation Programme under the Grant Agreement Number 857251 and by National Funds through FCT-Fundação para a Ciência e Tecnologia, under the scope of project UIDP/50027/2020.

## References

Bauer AM, de Silva A, Greenbaum E, Jackman T (2007) A new species of day gecko from high elevation in Sri Lanka, with a preliminary phylogeny of Sri Lankan *Cnemaspis* (Reptilia, Squamata, Gekkonidae). Mitteilungen aus dem Zoologischen Museum in Berlin 83: 22–32. https://doi.org/10.1002/mmnz.200600022

Bauer AM, Jackman TR, Greenbaum E, Giri VB, de Silva A (2010) South Asia supports a major endemic radiation of *Hemidactylus* geckos. Molecular Phylogenetics and Evolution 57(1): 343–352. https://doi.org/10.1016/j.ympev.2010.06.014

Benson DA, Cavanaugh M, Clark K, Karsch-Mizrachi I, Lipman DJ, Ostell J, Sayers EW (2013) GenBank. Nucleic Acids Research 41(D1): D36–D42. https://doi.org/10.1093/nar/gks1195

Bibi F, Kiessling W (2015) Continuous evolutionary change in Plio-Pleistocene mammals of eastern Africa. Proceedings of the National Academy of Sciences of the United States of America 112(34): 10623–10628. https://doi.org/10.1073/pnas.1504538112

Bittencourt-Silva G, Conradie W, Siu-Ting K, Tolley KA, Channing A, Cunningham M, Farooq HM, Menegon M, Loader SP (2016) The phylogenetic position and diversity of the enigmatic mongrel frog *Nothophryne* Poynton, 1963 (Amphibia, Anura). Molecular Phylogenetics and Evolution 99: 89–102. https://doi.org/10.1016/j.ympev.2016.03.021

Branch WR (1998) Field Guide to Snakes and other Reptiles of Southern Africa. Struik, Pretoria, 236 pp. https://doi.org/10.2307/1447414

Branch WR, Guyton JA, Schmitz A, Barej MF, Naskrecki P, Farooq H, Verburgt L, Rödel M-O (2017) Description of a new flat gecko (Squamata: Gekkonidae: *Afroedura*) from Mount Gorongosa, Mozambique. Zootaxa 4324(1): 142–160. https://doi.org/10.11646/zootaxa.4324.1.8

Branch WR, Schmitz A, Lobon-Rovira J, Baptista NL, Antônio T, Conradie W (2021) Rock island melody: A revision of the *Afroedura bogerti* Loveridge, 1944 group, with the description of four new endemic species from Angola. Zoosystematics and Evolution 97(1): 55–82. https://doi.org/10.3897/zse.97.57202

Briscoe NJ, Kearney MR, Taylor CA, Wintle BA (2016) Unpacking the mechanisms captured by a correlative species distribution model to improve predictions of climate refugia. Global Change Biology 22(7): 2425–2439. https://doi.org/10.1111/gcb.13280

Burbrink FT, Lawson R, Slowinski JB (2000) Mitochondrial DNA Phylogeography of the Polytypic North American Rat Snake (*Elaphe obsoleta*): A Critique of the Subspecies Concept. Evolution 54(6): 2107–2118. https://doi.org/10.1111/j.0014-3820.2000.tb01253.x

Busschau T, Conradie W, Daniels S (2019) Evidence for cryptic diversification in a rupicolous forest-dwelling gecko (Gekkonidae: *Afroedura pondolia*) from a biodiversity hotspot. Molecular Phylogenetics and Evolution 139: e106549. https://doi.org/10.1016/j.ympev.2019.106549

Candau JN, Fleming RA (2005) Landscape-scale spatial distribution of spruce budworm defoliation in relation to bioclimatic conditions. Canadian Journal of Forest Research 35(9): 2218–2232. https://doi.org/10.1139/x05-078

de Queiroz K (1998) The general lineage concept of species, species criteria, and the process of speciation: A conceptual unification and terminological recommendations. In: Howard DJ, Berlocher SH (Eds) Endless forms: Species and speciation. Oxford University Press, Oxford, 1–19.

deMenocal PB (2004) African climate change and faunal evolution during the Pliocene-Pleistocene. Earth and Planetary Science Letters 220(1–2): 3–24. https://doi.org/10.1016/S0012-821X(04)00003-2

Dirnböck T, Essl F, Rabitsch W (2011) Disproportional risk for habitat loss of high-altitude endemic species under climate change. Global Change Biology 17(2): 990–996. https://doi.org/10.1111/j.1365-2486.2010.02266.x

Enriquez-Urzelai U, Kearney MR, Nicieza AG, Tingley R (2019) Integrating mechanistic and correlative niche models to unravel range-limiting processes in a temperate amphibian. Global Change Biology 25(8): 2633–2647. https://doi.org/10.1111/gcb.14673

Feio M (1981) O relevo do sudoeste de Angola; estudo de geomorfologia. Memórias da Junta de Investigação Científica do Ultramar, Lisboa, 32 pp.

Fick SE, Hijmans RJ (2017) WorldClim 2: New 1–km spatial resolution climate surfaces for global land areas. International Journal of Climatology 37(12): 4302–4315. https://doi.org/10.1002/joc.5086

Griffin M (2002) Annotated Checklist and Provisional National Conservation Status of Namibian Reptiles. Technical Reports of Scientific Services. Number 1. Directorate of Scientific Services, Ministry of Environment and Tourism, Windhoek, 180 pp. https://www.lacerta.de/AF/Bibliografie/BIB_4908.pdf

Griffin M (2003) Annotated checklist and provisional national conservation status of Namibian reptiles. Namibia Scientific Society, Windhoek, 169 pp.

Hall TA (1999) BioEdit: a user-friendly biological sequence alignment editor and analysis program for Windows 95/98/NT. Nucleic Acids Symposium 41: 95–98.

Herrman H-W, Branch WR (2013) Fifty years of herpetological research in the Namib Desert and Namibia with an updated and annotated species checklist. Journal of Arid Environments 93: 94–115. https://doi.org/10.1016/j.jaridenv.2012.05.003

IUCN (2022) The IUCN Red List of Threatened Species. Version 2022-1. https://www.iucnredlist.org [Accessed on 28 September 2022]

Jacobsen NHG, Kuhn AL, Jackman TR, Bauer AM (2014) A phylogenetic analysis of the southern African gecko genus *Afroedura* Loveridge (Squamata: Gekkonidae), with the description of nine new species from Limpopo and Mpumalanga provinces of South Africa. Zootaxa 3846(4): 451–501. https://doi.org/10.11646/zootaxa.3846.4.1

Kumar S, Stecher G, Li M, Knyaz C, Tamura K (2018) MEGA X: Molecular Evolutionary Genetics Analysis across computing platforms. Molecular Biology and Evolution 35(6): 154–1549. https://doi.org/10.1093/molbev/msy096

Lanfear R, Frandsen PB, Wright AM, Senfeld T, Calcott B (2016) PartitionFinder 2: new methods for selecting partitioned models of evolution for molecular and morphological phylogenetic analyses. Molecular Biology and Evolution 34: 772–773.https://doi.org/10.1093/molbev/msw260

Makhubo BG, Tolley KA, Bates MF (2015) Molecular phylogeny of the *Afroedura nivaria* (Reptilia: Gekkonidae) species complex in South Africa provides insight on cryptic speciation. Molecular Phylogenetics and Evolution 82: 31–42. https://doi.org/10.1016/j.ympev.2014.09.025

Minh BQ, Schmidt HA, Chernomor O, Schrempf D, Woodhams MD, von Haeseler A, Lanfear R (2020) IQ-TREE 2: New Models and Efficient Methods for Phylogenetic Inference in the Genomic Era. Molecular Biology and Evolution 37(5): 1530–1534. https://doi.org/10.1093/molbev/msaa015

Nguyen L-T, Schmidt HA, von Haeseler A, Minh BQ (2015) IQ-TREE: A Fast and Effective Stochastic Algorithm for Estimating Maximum-Likelihood Phylogenies. Journal of Molecular Biology and Evolution 32(1): 268–274. https://doi.org/10.1093/molbev/msu300

Palumbi SR, Martin AP, Romano SL, McMillan WO, Stice L, Grabowski G (1991) The Simple Fool's Guide to PCR. Dept. ofZoology, University of Hawaii, Honolulu.

Rambaut A. 2014. FigTree version 1.4.4. http://tree.bio.ed.ac.uk/software/figtree/

Rambaut A, Drummond AJ, Xie D, Baele G, Suchard MA (2018) Posterior summarisation in Bayesian phylogenetics using Tracer 1.7. Systematic Biology 67(5): 901–904. https://doi.org/10.1093/sysbio/syy032

Reaney AM, Saldarriaga-Córdoba M, Pincheira-Donoso D (2018) Macroevolutionary diversification with limited niche disparity in a species-rich lineage of cold-climate lizards. BMC Evolutionary Biology 18(1): 1–12. https://doi.org/10.1186/s12862-018-1133-1

Ronquist F, Teslenko M, Van der Mark P, Ayres DL, Darling A, Höhna S, Larget B, Liu L, Suchard MA, Huelsenbeck JP (2012) MrBayes 3.2: Efficient Bayesian Phylogenetic Inference and Model Choice Across a Large Model Space. Systematic Biology 61(3): 539–542. https://doi.org/10.1093/sysbio/sys029

Stanley EL, Bauer AM, Jackman TR, Branch WR, Mouton LFN (2011) Between a rock and a hard polytomy: Rapid radiation in the rupicolous girdled lizards (Squamata: Cordylidae). Molecular Phylogenetics and Evolution 58(1): 53–70. https://doi.org/10.1016/j.ympev.2010.08.024

Thompson JD, Gibson TJ, Plewniak F, Jeanmougin F, Higgins DG (1997) The ClustalX windows interface: Flexible strategies for multiple sequence alignment aided by quality analysis tools. Nucleic Acids Research 24(24): 4876–4882. https://doi.org/10.1093/nar/25.24.4876

Uetz P, Freed P, Hošek J [Eds] (2022) The Reptile Database. http://www.reptile-database.org [Accessed 11 April 2021]

Wiens JJ, Kuczynski CA, Townsend T, Reeder TW, Mulcahy DG, Sites Jr JW (2010) Combining Phylogenomics and Fossils in Higher-Level Squamate Reptile Phylogeny: Molecular Data Change the Placement of Fossil Taxa. Systematic Biology 59(6): 674–688. https://doi.org/10.1093/sysbio/syq048

Yang XQ, Kushwaha SPS, Saran S, Xu J, Roy PS (2013) Maxent modeling for predicting the potential distribution of medicinal plant, *Justicia adhatoda* L. in Lesser Himalayan foothills. Ecological Engineering 51: 83–87. https://doi.org/10.1016/j.ecoleng.2012.12.004

Zhang D, Gao F, Jakovlić I, Zou H, Zhang J, Li WX, Wang GT (2020) PhyloSuite: An integrated and scalable desktop platform for streamlined molecular sequence data management and evolutionary phylogenetics studies. Molecular Ecology Resources 20(1): 348–355. https://doi.org/10.1111/1755-0998.13096